ISSN 2720-3581

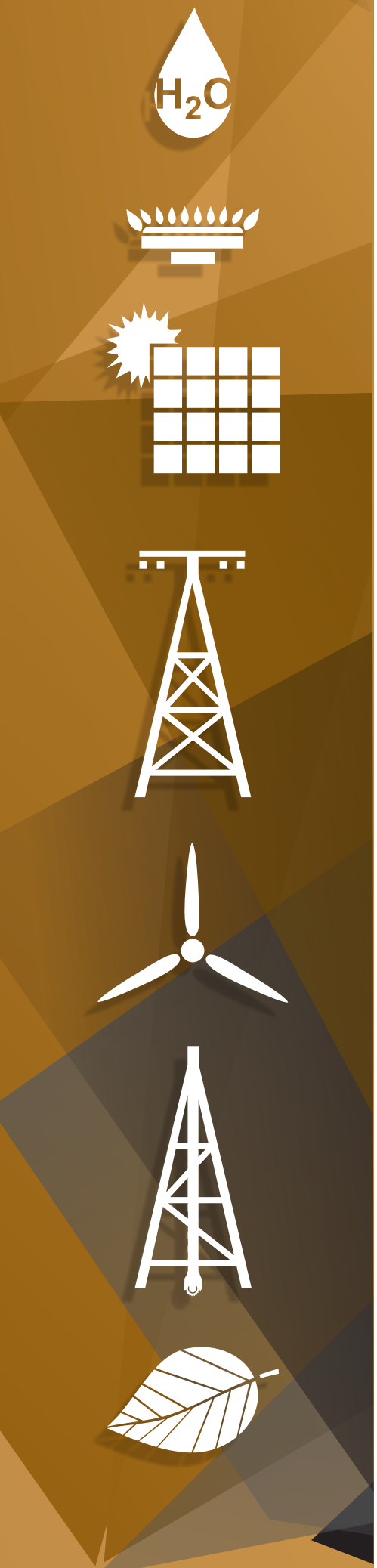

JOURNAL OF GEOTECHNOLOGY AND ENERGY

FORMERLY AGH DRILLING, OIL, GAS

2025, vol. 42, no. 1

WYDAWNICTWA AGH

KRAKOW 2025

ISSN 2720-3581

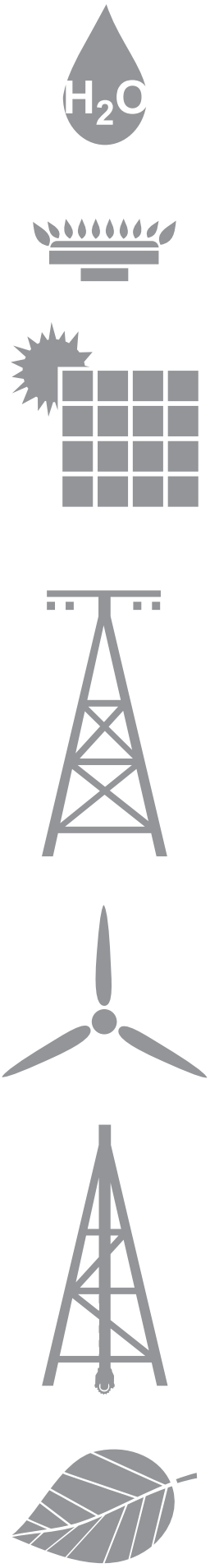

JOURNAL OF GEOTECHNOLOGY AND ENERGY

FORMERLY AGH DRILLING, OIL, GAS

2025, vol. 42, no. 1

WYDAWNICTWA AGH

KRAKOW 2025

The "Journal of Geotechnology and Energy" (formerly "AGH Drilling, Oil, Gas") is a quarterly published by the Faculty of Drilling, Oil and Gas at the AGH University of Krakow, Poland. Journal is an interdisciplinary, international, peer-reviewed, and open access. The articles published in JGE have been given a favorable opinion by the reviewers designated by the editorial board.

Editorial Team

Publisher

AGH University Press

Linguistic corrector: *Aeddan Shaw*
Technical editor: *Kamila Zimnicka*
Desktop publishing: *Munda*
Cover design: *Paweł Sepielak*

ISSN: 2720-3581
DOI: https://doi.org/10.7494/jge

Journal website: https://journals.agh.edu.pl/jge

Wydawnictwa AGH (AGH University Press)
al. A. Mickiewicza 30, 30-059 Kraków
tel. 12 617 32 28, 12 636 40 38
e-mail: redakcja@wydawnictwoagh.pl
www.wydawnictwo.agh.edu.pl

CONTENTS

Journal of Geotechnology and Energy | vol. 42 | no. 1 | 2025 | pp. 21–26

https://doi.org/10.7494/jge.2025.42.1.7010

ARTICLE

POTENTIAL APPLICATIONS OF THE VOM BERG RHEOLOGICAL MODEL IN RESEARCH ON POLYMER-MODIFIED DRILLING MUDS

Krzysztof Skrzypaszek

AGH University of Krakow, Faculty of Drilling, Oil and Gas, Poland
ORCID: 0000-0003-2358-7361
e-mail: varna@agh.edu.pl

Date of submission:
16.02.2025

Date of acceptance:
25.02.2025

Date of publication:
31.03.2025

https://journals.agh.edu.pl/jge

Abstract: This article examines the potential applications of the Vom Berg rheological model in the technology of polymer-modified drilling muds. In recent years, intensive research has been conducted at the Faculty of Drilling, Oil, and Gas to optimize procedures for selecting rheological models for technological fluids used in drilling operations. One of the key outcomes of this research is the proprietary RheoSolution methodology, applied in this study to assess the adaptability of the Vom Berg rheological model. Originally developed for analyzing the rheology of cement slurries in civil engineering, this model has been utilized here to describe the relationship between shear stress and shear rate in polymer-modified drilling muds. As part of the research, laboratory experiments were conducted at the Drilling Fluids Laboratory of the Faculty of Drilling, Oil, and Gas, focusing on drilling muds modified with xanthan biopolymer. The obtained results served as the basis for a comparative analysis of the classical API methodology and the proposed RheoSolution approach in determining the rheological parameters of the tested fluids. Special attention was given to the applicability of the Vom Berg model as a tool for a more precise characterization of drilling mud behavior under dynamic conditions. This article is part of a broader series of publications aimed at demonstrating the utility and potential advantages of the RheoSolution methodology in studies on the rheological properties of technological drilling muds.

Keywords: drilling, drilling muds, drilling fluids, rheology, Vom Berg, RheoSolution

1. Introduction

Rheological modeling plays a fundamental role in the study of drilling fluids, as it directly influences the accuracy of flow resistance calculations in a closed-loop circulation system. Proper determination of the relationship between shear stress and shear rate is essential for assessing the hydraulic parameters of drilling operations, particularly in terms of fluid transport efficiency, wellbore stability, and cuttings removal. The precise estimation of flow resistance enables the optimization of key drilling infrastructure elements, such as mud pumps, and contributes to the overall efficiency and safety of drilling operations. The ability to accurately characterize the rheological behavior of drilling fluids is therefore a crucial aspect of optimizing their formulation and ensuring their effective performance under various wellbore conditions.

In practical drilling applications, rheological models recommended by the American Petroleum Institute Recommended Practice 13 (API RP 13) are widely used. These models range from linear models, such as the Bingham Plastic model, to power-law models, such as the Ostwald-de Waele model [1]. While these models provide useful approximations, their ability to accurately describe the complex behavior of modified drilling fluids remains limited. Many modern drilling fluids, particularly those enhanced with polymeric additives or nanoparticles, exhibit non-Newtonian behavior that deviates from the assumptions underlying these conventional models. As a result, there is a growing need for alternative approaches that can offer more accurate and flexible representations of drilling fluid rheology, particularly for fluids that undergo structural modifications under different shear conditions. One of the key rheological parameters that play a significant role in the evaluation of drilling fluids is yield point. This parameter defines the minimum shear stress required to initiate fluid flow and is particularly crucial in drilling applications, as it determines the ability of the fluid to suspend and transport cuttings, maintain wellbore stability, and prevent solid phase sedimentation. Traditional models, such as the Bingham Plastic model, incorporate yield point as a primary characteristic, however, their simplified nature often leads to inaccuracies in predicting the behavior of complex drilling fluids, especially those exhibiting structural transformations under dynamic conditions. A more advanced rheological model capable of capturing these changes could significantly improve the accuracy of hydraulic calculations and contribute to more effective drilling fluid design.

The Vom Berg rheological model originates from extensive research conducted in the 1990s on cement slurries used in construction, which naturally led to its application in cement slurry technologies for wellbore cementing [2]. The need for a more accurate description of cementitious materials, which often exhibit complex flow properties due to their time-dependent structural evolution, motivated the development of multi-parameter rheological models such as the Vom Berg equation. Given the similarities between cement slurries used in construction and those employed in oil and gas well cementing, the model gained interest in the drilling industry. However, the author of this article has observed that the Vom Berg model also provides excellent correlation when applied to polymer-modified drilling fluids, in contrast to conventional bentonite-based drilling fluids, where linear models such as the Bingham Plastic model (recommended by API) have been successfully used. This suggests that the Vom Berg model may have broader applicability in the study of advanced, chemically modified drilling fluids.

In the following sections, the author aims to demonstrate that, by utilizing the classical methodology for selecting rheological models based on rheological measurements performed with a FANN 12-speed viscometer, it is possible to successfully apply the Vom Berg equation to improve the accuracy of describing the relationship between shear stress and shear rate [3]. By comparing the results obtained from traditional models with those provided by the Vom Berg model, this study highlights its potential advantages in refining the characterization of drilling fluid behavior. This improvement in rheological characterization justifies the use of the Vom Berg model as a reliable tool for analyzing the flow properties of modified drilling fluids, particularly those enhanced with polymeric additives. The findings presented in this paper aim to contribute to the development of more precise methodologies for rheological analysis in drilling fluid technology, ultimately leading to better fluid performance and enhanced drilling efficiency.

2. The RheoSolution methodology and its application in research on the rheology of technological drilling fluids

The methodology employed regression analysis to model the relationship between shear stress and shear rate, while the Pearson linear correlation coefficient was used as a comparative criterion. In the case of mathematically simple rheological models: Bingham's linear model and Ostwald–de Waele's exponential model, the rheological parameters can be determined in a relatively straightforward analytical manner.

In the case of linear regression, the optimal function is predicted in the form of a linear equation:

$$\hat{y} = ax + b \tag{1}$$

The least squares condition is specified in the following form:

$$U = \sum_{i=1}^{m} (y_i - \hat{y})^2 \rightarrow \min \tag{2}$$

After incorporating the dependencies, the following expression is obtained:

$$U = \sum_{i=1}^{m} (y_i^2 - 2ax_i y_i - 2by_i + a^2 x_i^2 + 2abx_i + b^2) \rightarrow \min \tag{3}$$

The above equation is a function of the coefficients a and b. Therefore, the condition for minimizing the function U can be expressed in the form of the following equations:

$$\begin{cases} \dfrac{\partial U}{\partial a} = -2\sum_{i=1}^{m} x_i y_i + 2a\sum_{i=1}^{m} x_i^2 + 2b\sum_{i=1}^{m} x_i = 0 \\ \dfrac{\partial U}{\partial b} = -2\sum_{i=1}^{m} y_i + 2a\sum_{i=1}^{m} x_i + 2bm = 0 \end{cases} \tag{4}$$

Solving this system of equations yields the well-known formulas for linear regression coefficients found in the literature [4, 5]:

$$a = \frac{m\sum_{i=1}^{m} x_i y_i - \sum_{i=1}^{m} x_i \sum_{i=1}^{m} y_i}{m\sum_{i=1}^{m} x_i^2 - \left(\sum_{i=1}^{m} x_i\right)^2} \tag{5}$$

$$b = \frac{\sum_{i=1}^{m} y_i - a\sum_{i=1}^{m} x_i}{m} \tag{6}$$

The use of regression analysis (1)–(6) to determine the reological parameters of selected rheological models is as follows:

– **The Bingham model** is a linear model of a plastic body that, in a resting state, maintains a three-dimensional structure with a certain degree of elasticity. Once this elasticity – known as the yield stress or plastic limit – is exceeded, the material begins to flow. The yield stress represents the intermolecular forces present in the fluid. After surpassing this threshold, a Bingham body exhibits its characteristics of a Newtonian fluid, where stress propagates in direct proportion to the forces causing it, following a linear relationship [6].

This model is described by two parameters and represents the first modification of Newton's model. Due to its simplicity, it has been widely used as a fundamental rheological model for decades.

Assuming the rheological model of Bingham fluid in the form of:

$$\tau = \tau_y + \eta \cdot \dot{\gamma} \tag{7}$$

and substituting $\eta = a$, $\tau_y = b$, $\dot{\gamma} = x$ and $\tau = y$ the following relationship is obtained:

$$\hat{y} = ax + b \tag{8}$$

next, the rheological parameters of the Bingham fluid can be determined as follows:

$$\eta = \frac{m\sum_{i=1}^{m} x_i y_i - \sum_{i=1}^{m} x_i \sum_{i=1}^{m} y_i}{m\sum_{i=1}^{m} x_i^2 - \left(\sum_{i=1}^{m} x_i\right)^2} \tag{9}$$

$$\tau_y = \frac{\sum_{i=1}^{m} y_i - a\sum_{i=1}^{m} x_i}{m} \tag{10}$$

– **The power-law model**, also known as the Ostwald–de Waele model, describes a pseudoplastic body. This model was introduced after it was observed that the resulting curve closely resembles a straight line on a plot of shear stress versus shear rate with both axes in logarithmic scale, the resulting curve closely resembles a straight line. It is a two-parameter model that effectively describes the behavior of most fluids, particularly shear-thinning fluids. However, it does not account for the yield stress, which is a limitation of the model [7].

Approximating the given fluid using the Ostwald–de Waele model:

$$\tau = k \cdot \dot{\gamma}^n \tag{11}$$

the calculation procedure requires linearization of the above relationship into the following form:

$$\hat{y} = ax + b \tag{12}$$

this is achieved by taking the logarithm of both sides of the equation:

$$\ln\tau = \ln k + n\ln\dot{\gamma} \tag{13}$$

and substituting: $n = a$, $\ln k = b$, $\ln\dot{\gamma} = x$, $\ln\tau = y$.

Next, the rheological parameters of the Ostwald–de Waele model are determined as follows:

$$n = \frac{m\sum_{i=1}^{m} x_i y_i - \sum_{i=1}^{m} x_i \sum_{i=1}^{m} y_i}{m\sum_{i=1}^{m} x_i^2 - \left(\sum_{i=1}^{m} x_i\right)^2} \tag{14}$$

$$k = e^{\left(\frac{\sum_{i=1}^{m} y_i - a\sum_{i=1}^{m} x_i}{m}\right)} \tag{15}$$

– **The multiparameter Vom Berg model** is presented in the form of the following equation:

$$\tau = \tau_y + B\sinh^{-1}\left(\frac{-\frac{dv}{dr}}{C}\right) \tag{16}$$

the least squares method applied to the Vom Berg model is formulated as follows:

$$\begin{aligned} U &= \sum_{i=1}^{m}\left(y_i - \left(a + b\sinh^{-1}\left(\frac{x_i}{c}\right)\right)\right)^2 = \\ &= \sum_{i=1}^{m}\left(y_i^2 - 2ay_i - 2y_i b\sinh^{-1}\left(\frac{x_i}{c}\right) + a^2 + \right. \\ &\left. +2ab\sinh^{-1}\left(\frac{x_i}{c}\right) + b^2\left(\sinh^{-1}\left(\frac{x_i}{c}\right)\right)^2\right) \to \min \end{aligned} \tag{17}$$

the partial derivatives of the parameters a, b, and c form the following system of equations:

$$\begin{aligned} \frac{\partial U}{\partial a} &= 2\sum_{i=1}^{m}\left(b\sinh^{-1}\left(\frac{x_i}{c}\right)\right) - 2\sum_{i=1}^{m} y_i + 2am = 0 \\ \frac{\partial U}{\partial b} &= \sum_{i=1}^{m}\left[-2\sinh^{-1}\left(\frac{x_i}{c}\right)\left(-a - b\sinh^{-1}\left(\frac{x_i}{c}\right) + y_i\right)\right] = 0 \\ \frac{\partial U}{\partial c} &= \sum_{i=1}^{m}\frac{2bx_i\left(-a - b\sinh^{-1}\left(\frac{x_i}{c}\right) + y_i\right)}{c^2\sqrt{1+\frac{x_i^2}{c^2}}} = 0 \end{aligned} \tag{18}$$

The above system of equations cannot be solved analytically, as such an attempt leads to an implicit equation involving a single variable. Consequently, a numerical approach was developed to determine the parameters of the Vom Berg model. For this purpose, the simple gradient method, previously described in the author's earlier works, was applied. This method is relatively straightforward to implement and computationally efficient for solving nonlinear equations. It is based on defining and computing a partial derivative vector, which aligns with the error function gradient but moves in the opposite direction. The algorithm iterates along this direction as long as the error function value decreases. Once the function ceases to decrease, a new vector is computed [8–11].

In this case, the vector is three-dimensional, with a unit length set to 1 to accelerate calculations. The error function, where the parameters x, y, and z represent the rheological parameters of the model, is formulated as follows:

$$U(x,y,z) = \sum_{i=0}^{n}\left(f(x,y,z) - y_i\right)^2 \to \min \tag{19}$$

the vector follows the direction of the error function gradient but has an opposite orientation, with a length equal to 1:

$$\hat{v} = \frac{-\vec{\nabla}U}{\left|-\vec{\nabla}U\right|} \tag{20}$$

as a result of numerical calculations, the final vector is obtained:

$$\vec{v} = (x, y, z) \tag{21}$$

whose values are:

$$\begin{aligned} \tau &= \tau_y + B\sinh^{-1}\left(\frac{-\frac{dv}{dr}}{C}\right) \\ \tau_y &= v_x \\ B &= v_y \\ C &= v_z \end{aligned} \tag{22}$$

In the RheoSolution methodology, statistical criteria are applied to assess the quality of the model's fit to the measurement data:

– the sum of squared differences:

$$U = \sum_{i=1}^{m}\left(y_i - \hat{y}\right)^2 \tag{23}$$

– Pearson linear correlation coefficient:

$$R = \sqrt{1 - \frac{U}{\sum_{i=1}^{m}\left(y_i - \overline{y}\right)^2}} = \sqrt{1 - \frac{\sum_{i=1}^{m}\left(y_i - \hat{y}\right)^2}{\sum_{i=1}^{m}\left(y_i - \overline{y}\right)^2}} \tag{24}$$

– Fischer–Sneadecor coefficient:

$$F = \frac{R^2}{1 - mR^2} \tag{25}$$

The above methodology is implemented in the RheoSolution software and has been used in the interpretation of laboratory results presented in the next chapter (Tabs. 1–18, Figs. 1–9).

3. Laboratory studies conducted at the Faculty of Drilling, Oil, and Gas

To evaluate the applicability of the Vom Berg rheological model in describing the rheological properties of polymer-modified drilling muds, a series of laboratory experiments were conducted at the Drilling Fluids Laboratory of the Faculty of Drilling, Oil, and Gas. The primary objective was to compare the effectiveness of the Vom Berg model with the widely used Bingham and Ostwald–de Waele models recommended by API.

The compositions of the tested drilling muds were developed in collaboration with Polski Serwis Płynów Wiertniczych Sp. z o.o. (PSPW Krosno), a company specializing in drilling fluid services. This cooperation ensured that the tested mud formulations closely resembled real-world drilling fluid systems used in industrial applications.

The study involved nine drilling mud samples, each with a different composition:

– Sample 1 – A base bentonite mud containing only water and 5% Bentopol Żebiec bentonite, serving as the control sample.
– Sample 2 – The base mud with 0.1% xanthan biopolymer, used to assess the impact of biopolymer addition on rheology.
– Sample 6 – The base mud with 0.3% xanthan biopolymer, allowing evaluation of the effect of increased biopolymer concentration.
– Samples 3, 4, 5, 7, 8, and 9 – Mud formulations incorporating additional rheological additives such as Alcomer and Desco [12, 13], commonly used in the drilling industry to enhance stability and control filtration properties. These additives were included to replicate industrial drilling mud formulations and assess their influence on rheological model fitting.

Rheological measurements were conducted using a FANN 12-speed rotational viscometer, recommended by API [1]. The data obtained from these experiments were processed and analyzed using RheoSolution 5.0, a proprietary software based on the RheoSolution methodology developed by Prof. Rafał Wiśniowski and the author of this study [14]. This advanced tool facilitated precise rheological model fitting and comprehensive evaluation of their effectiveness in describing the properties of the tested drilling muds. The results, presented in the following sections in the form of tables and graphs, highlight the extent to which the Vom Berg model outperforms API-recommended models in capturing the rheological behavior of polymer-modified drilling muds. Special emphasis was placed on comparing the performance of each model across different shear rate ranges, providing insight into their suitability for various operational conditions in drilling technology.

For simplicity and better readability of the graphs, their axes are labeled with the Greek letters $\boldsymbol{\tau}$, representing shear stress [Pa], and $\boldsymbol{\gamma}$, denoting shear rate ($-dv/dr$) with the unit 1/s.

Table 1. Results of rheological measurements for sample No. 1 (Bentonite 5% without the addition)

Rotor speed [rot/min]	Angle [o]	Shear rate [1/s]	Shear stress [Pa]
600	28	1 022.040	14.299
300	20	511.020	10.214
200	17	340.680	8.682
100	14	170.340	7.149
60	12	102.204	6.128
30	11	51.102	5.617
20	10	34.068	5.107
10	10	17.034	5.107
6	9	10.220	4.596
3	9	5.110	4.596
2	8	3.406	4.085
1	8	1.703	4.085

Table 2. Summary of correlation coefficients of the analyzed rheological models for sample No. 1

Rheological model	Pearson correlation coefficient, *R*	Fischer–Sneadecor coefficient, *F*	Sum of squares, *U*
Bingham	0.987	377.93	2.66
Ostwald–de Waele	0.921	54.99	15.88
Vom Berg	0.953	102.99	9.14

The determined rheological parameters of the Vom Berg model for sample No. 1: parameter B = 2.22 Pa·s, parameter C = 45.36 [–], parameter YP = 3.74 Pa.

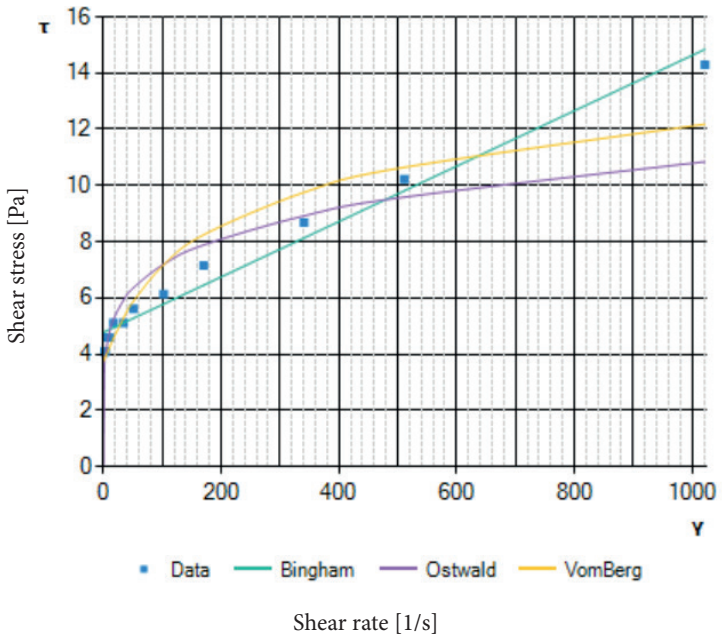

Fig. 1. Comparison of the Vom Berg model with the Bingham and Ostwald–de Waele model (API) for sample No. 1

Table 3. Results of rheological measurements for sample No. 2
(Bentonite 5% with the addition of 0.1% xanthan gum biopolymer (BWOC))

Rotor speed [rot/min]	Angle [o]	Shear rate [1/s]	Shear stress [Pa]
600	54	1 022.040	27.577
300	42	511.020	21.448
200	35	340.680	17.874
100	26	170.340	13.278
60	22	102.204	11.235
30	19	51.102	9.703
20	18	34.068	9.192
10	16	17.034	8.171
6	15	10.220	7.661
3	14	5.110	7.149
2	14	3.406	7.149
1	13	1.703	6.639

Table 4. Summary of correlation coefficients of the analyzed rheological models for sample No. 2

Rheological model	Pearson correlation coefficient, *R*	Fischer–Sneadecor coefficient, *F*	Sum of squares, *U*
Bingham	0.973	177.91	26.09
Ostwald–de Waele	0.944	81.89	53.36
Vom Berg	0.998	2 257.38	2.16

Determined rheological parameters of the Vom Berg model for sample No. 2: parameter B = 8.15 Pa·s, parameter C = 177.45 [–], parameter YP = 7.01 Pa.

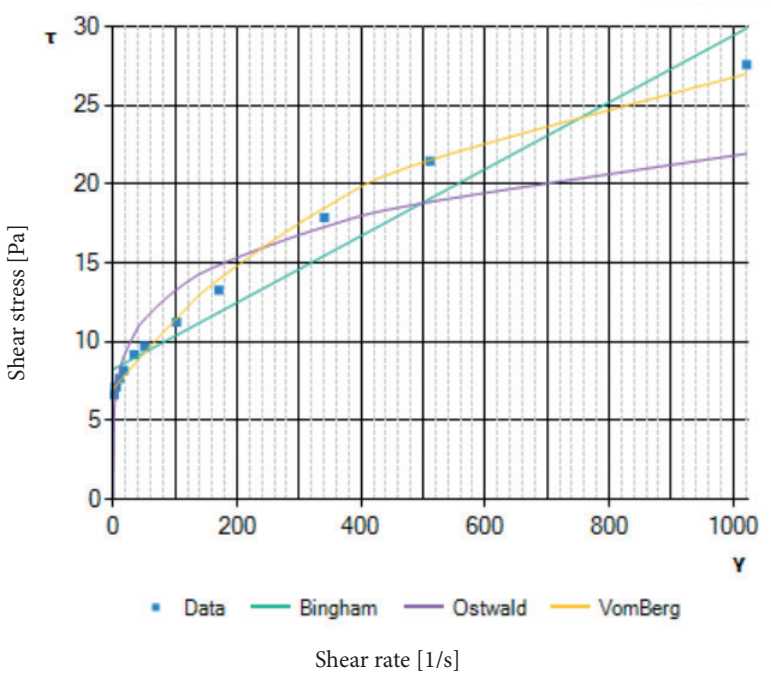

Fig. 2. Comparison of the Vom Berg model with the Bingham and Ostwald–de Waele model (API) for sample No. 2

Table 5. Results of rheological measurements for sample No. 3

Rotor speed [rot/min]	Angle [o]	Shear rate [1/s]	Shear stress [Pa]
600	133	1 022.040	67.920
300	102	511.020	52.089
200	88	340.680	44.940
100	70	170.340	35.747
60	62	102.204	31.662
30	54	51.102	27.577
20	51	34.068	26.045
10	47	17.034	24.002
6	44	10.220	22.470
3	40	5.110	20.427
2	37	3.406	18.895
1	28	1.703	14.299

Table 6. Summary of correlation coefficients of the analyzed rheological models for sample No. 3 (Bentonite 5% with the addition of 0.1% xanthan gum biopolymer and Alcomer 0.02% (BWOC))

Rheological model	Pearson correlation coefficient, R	Fischer–Sneadecor coefficient, F	Sum of squares, U
Bingham	0.950	116.453	213.82
Ostwald–de Waele	0.970	161.603	157.56
Vom Berg	0.985	312.740	83.77

Determined rheological parameters of the Vom Berg model for sample No. 3: parameter B = 14.06 Pa·s, parameter C = 84.03 [–], parameter YP = 18.43 Pa.

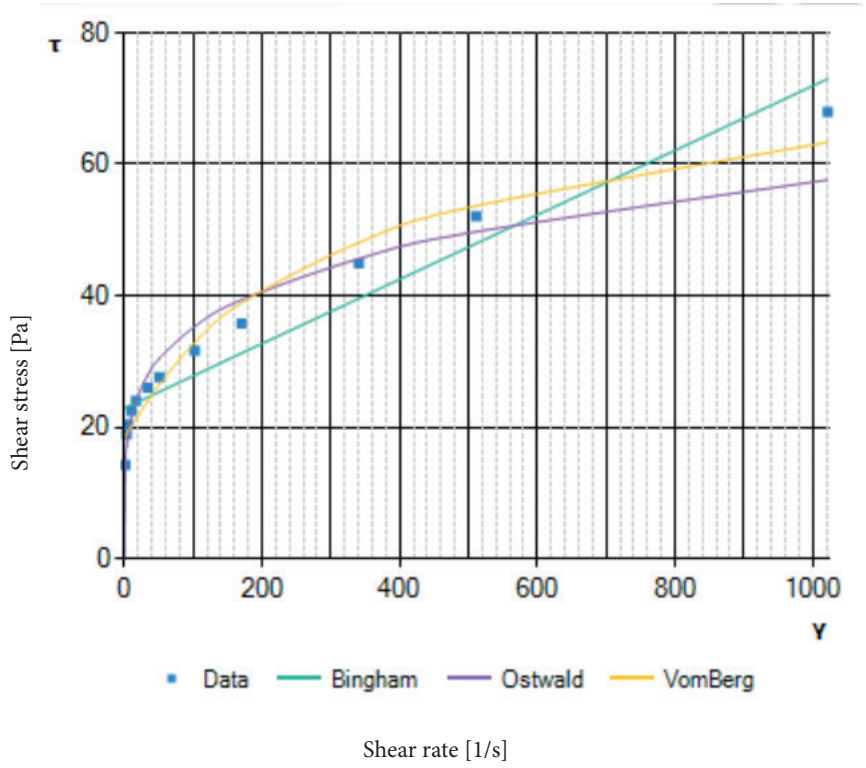

Fig. 3. Comparison of the Vom Berg model with the Bingham and Ostwald–de Waele model (API) for sample No. 3

Table 7. Results of rheological measurements for sample No. 4
(Bentonite 5% with the addition of 0.1% xanthan gum biopolymer and Alcomer 0.02% + Desco 0.1% (BWOC))

Rotor speed [rot/min]	Angle [o]	Shear rate [1/s]	Shear stress [Pa]
600	84	1 022.040	42.897
300	62	511.020	31.662
200	53	340.680	27.066
100	41	170.340	20.938
60	35	102.204	17.874
30	30	51.102	15.320
20	28	34.068	14.299
10	24	17.034	12.256
6	22	10.220	11.235
3	20	5.110	10.214
2	19	3.406	9.703
1	17	1.703	8.682

Table 8. Summary of correlation coefficients of the analyzed rheological models for sample No. 4

Rheological model	Pearson correlation coefficient, *R*	Fischer–Sneadecor coefficient, *F*	Sum of squares, *U*
Bingham	0.969	155.354	73.18
Ostwald–de Waele	0.965	137.213	82.20
Vom Berg	0.980	238.580	48.68

Determined rheological parameters of the Vom Berg model for sample No. 4: parameter B = 7.96 Pa·s, parameter C = 49.20 [–], parameter YP = 8.49 Pa.

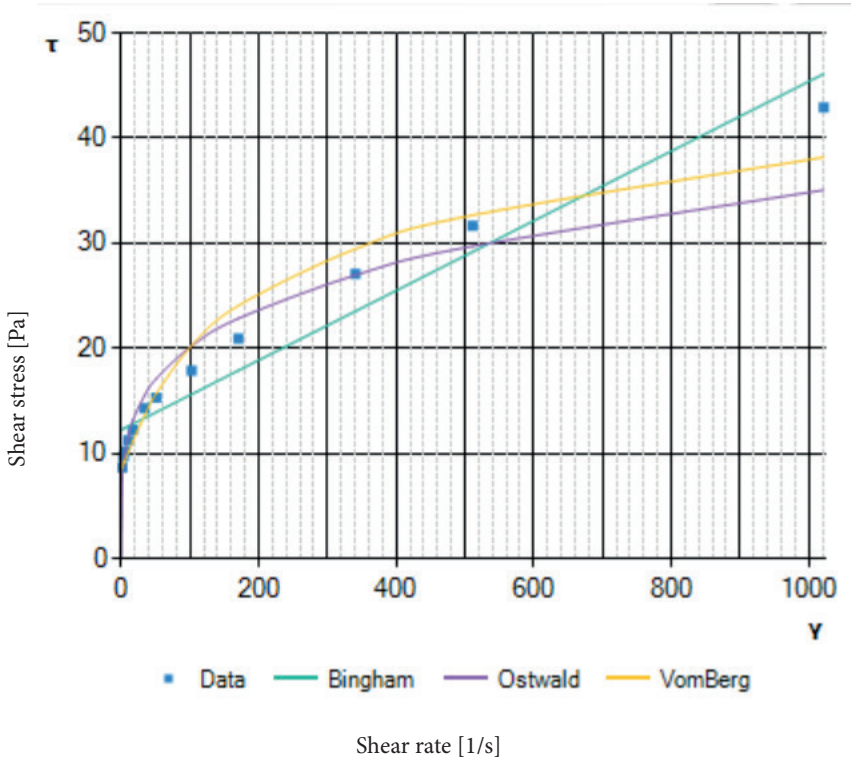

Fig. 4. Comparison of the Vom Berg model with the Bingham and Ostwald–de Waele model (API) for sample No. 4

Table 9. Results of rheological measurements for sample No. 5
(Bentonite 5% with the addition of 0.1% xanthan gum biopolymer and Alcomer 0.02% + Desco 0.2% (BWOC))

Rotor speed [rot/min]	Angle [o]	Shear rate [1/s]	Shear stress [Pa]
600	74	1 022,040	60,260
300	53	511,020	39,833
200	44	340,680	31,151
100	33	170,340	22,981
60	27	102,204	18,895
30	22	51,102	14,810
20	19	34,068	13,278
10	17	17,034	10,214
6	15	10,220	7,660
3	14	5,110	5,107
2	13	3,406	4,085
1	11	1,703	3,064

Table 10. Summary of correlation coefficients of the analyzed rheological models for sample No. 5

Rheological model	Pearson correlation coefficient, R	Fischer–Sneadecor coefficient, F	Sum of squares, U
Bingham	0.973	183.920	55.63
Ostwald–de Waele	0.965	135.854	73.97
Vom Berg	0.979	219.938	46.92

Determined rheological parameters of the Vom Berg model for sample No. 5: parameter B = 7.57 Pa·s, parameter C = 50.64 [–], parameter YP = 5.15 Pa.

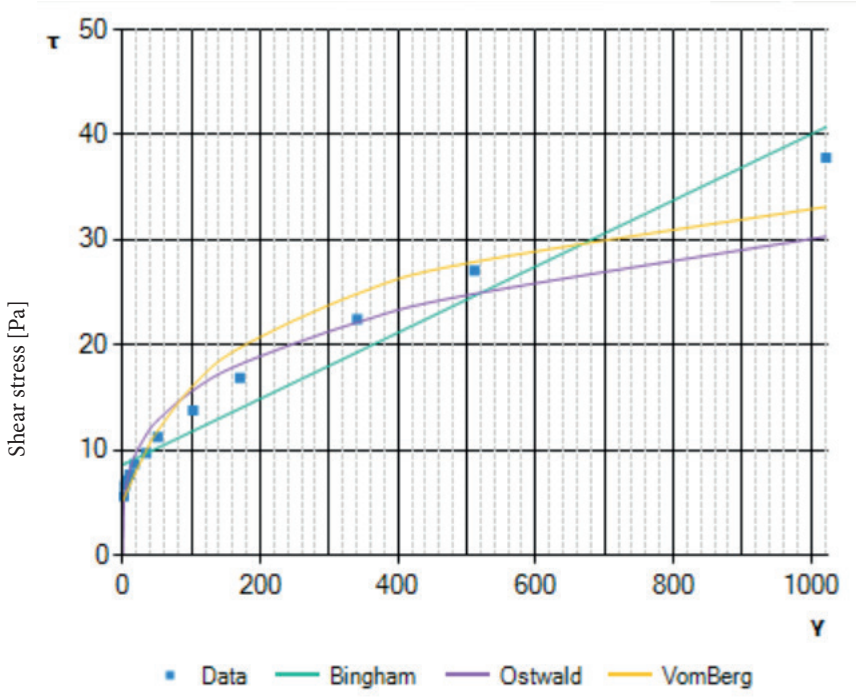

Fig. 5. Comparison of the Vom Berg model with the Bingham and Ostwald–de Waele model (API) for sample No. 5

Table 11. Results of rheological measurements for sample No. 6 (Bentonite 5% with the addition of 0.3% xanthan gum (BWOC))

Rotor speed [rot/min]	Angle [o]	Shear rate [1/s]	Shear stress [Pa]
600	100	1 022.040	51.068
300	73	511.020	37.279
200	62	340.680	31.662
100	48	170.340	24.513
60	41	102.204	20.938
30	35	51.102	17.874
20	32	34.068	16.342
10	28	17.034	14.299
6	26	10.220	13.278
3	24	5.110	12.256
2	22	3.406	11.235
1	20	1.703	10.214

Table 12. Summary of correlation coefficients of the analyzed rheological models for sample No. 6

Rheological model	Pearson correlation coefficient, *R*	Fischer–Sneadecor coefficient, *F*	Sum of squares, *U*
Bingham	0.972	174.430	92.85
Ostwald–de Waele	0.961	122.132	129.61
Vom Berg	0.994	734.043	23.01

Determined rheological parameters of the Vom Berg model for sample No. 6: parameter B = 14.13 Pa·s, parameter C = 151.03 [–], parameter YP = 11.73 Pa.

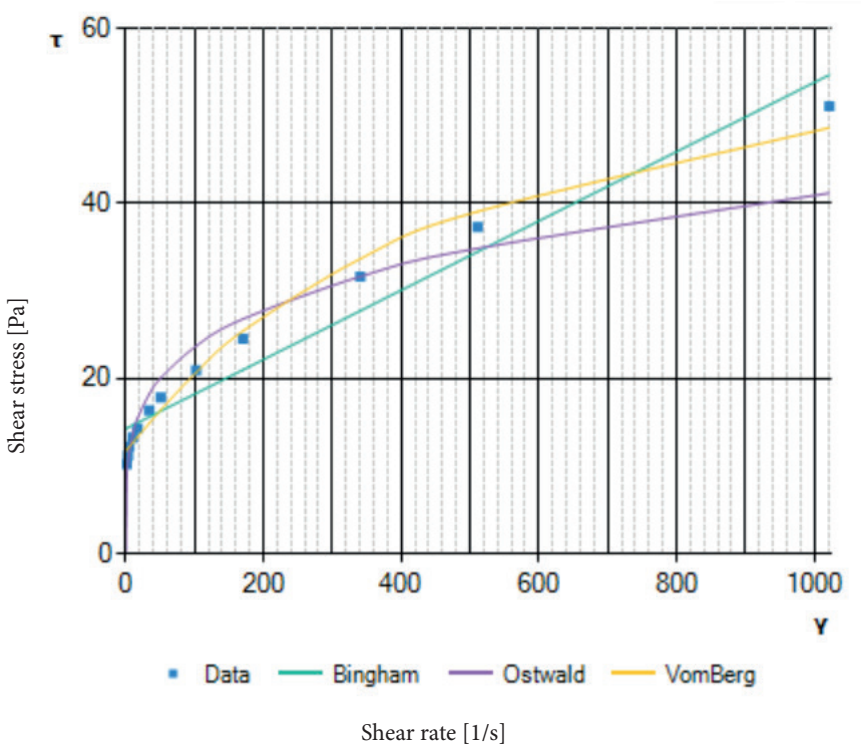

Fig. 6. Comparison of the Vom Berg model with the Bingham and Ostwald–de Waele model (API) for sample No. 7

Table 13. Results of rheological measurements for sample No. 7
(Bentonite 5% with the addition of 0.3% xanthan gum and Alcomer 0.01% (BWOC)

Rotor speed [rot/min]	Angle [o]	Shear rate [1/s]	Shear stress [Pa]
600	146	1 022.040	74.559
300	115	511.020	58.728
200	99	340.680	50.557
100	82	170.340	41.876
60	75	102.204	38.301
30	68	51.102	34.726
20	63	34.068	32.173
10	58	17.034	29.619
6	53	10.220	27.066
3	46	5.110	23.491
2	41	3.406	20.938
1	37	1.703	18,895

Table 14. Summary of correlation coefficients of the analyzed rheological models for sample No. 7

Rheological model	Pearson correlation coefficient, *R*	Fischer–Sneadecor coefficient, *F*	Sum of squares, *U*
Bingham	0.946	85.680	317.48
Ostwald–de Waele	0.979	241.592	120.74
Vom Berg	0.982	261.863	111.74

Determined rheological parameters of the Vom Berg model for sample No. 7: parameter B = 13.71 Pa·s, parameter C = 65.38 [–], parameter YP = 22.42 Pa.

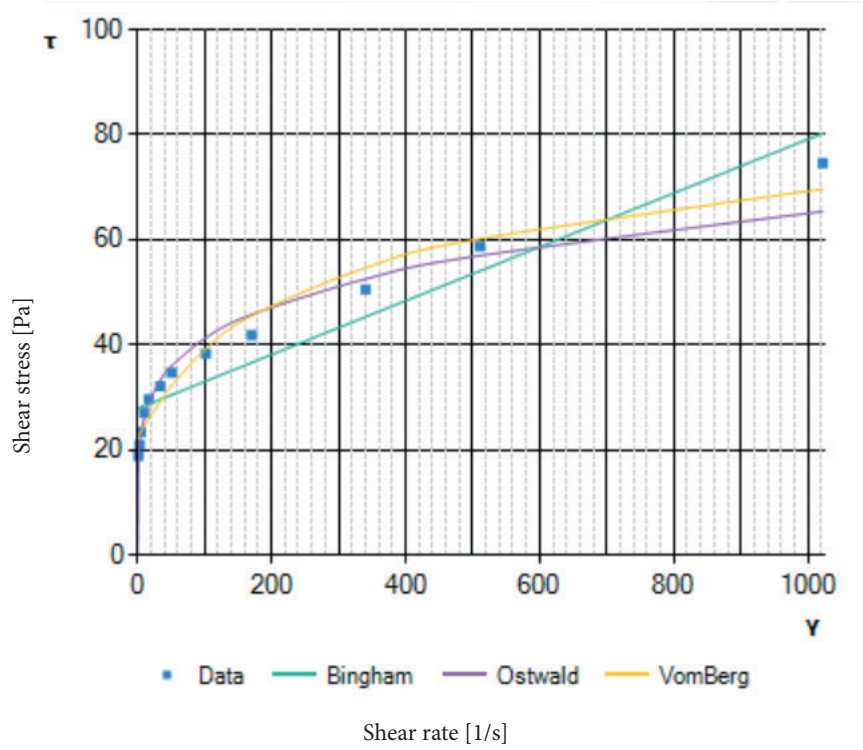

Fig. 7. Comparison of the Vom Berg model with the Bingham and Ostwald–de Waele model (API) for sample No. 7

Table 15. Results of rheological measurements for sample No. 8
(Bentonite 5% with the addition of 0.3% xanthan gum and Alcomer 0.02% + Desco 0.1% (BWOC))

Rotor speed [rot/min]	Angle [o]	Shear rate [1/s]	Shear stress [Pa]
600	118	1 022.040	60,260
300	91	511.020	46.472
200	78	340.680	39.833
100	62	170.340	31.662
60	54	102.204	27.577
30	46	51.102	23.491
20	43	34.068	21.959
10	38	17.034	19.406
6	35	10.220	17.874
3	33	5.110	16.852
2	31	3.406	15.831
1	28	1.703	14.299

Table 16. Summary of correlation coefficients of the analyzed rheological models for sample No. 8

Rheological model	Pearson correlation coefficient, *R*	Fischer–Sneadecor coefficient, *F*	Sum of squares, *U*
Bingham	0.963	129.356	159.93
Ostwald–de Waele	0.966	143.513	145.18
Vom Berg	0.996	997.096	22.13

Determined rheological parameters of the Vom Berg model for sample No. 8: parameter B = 16.23 Pa·s, parameter C = 152.80 [–], parameter YP = 16.54 Pa.

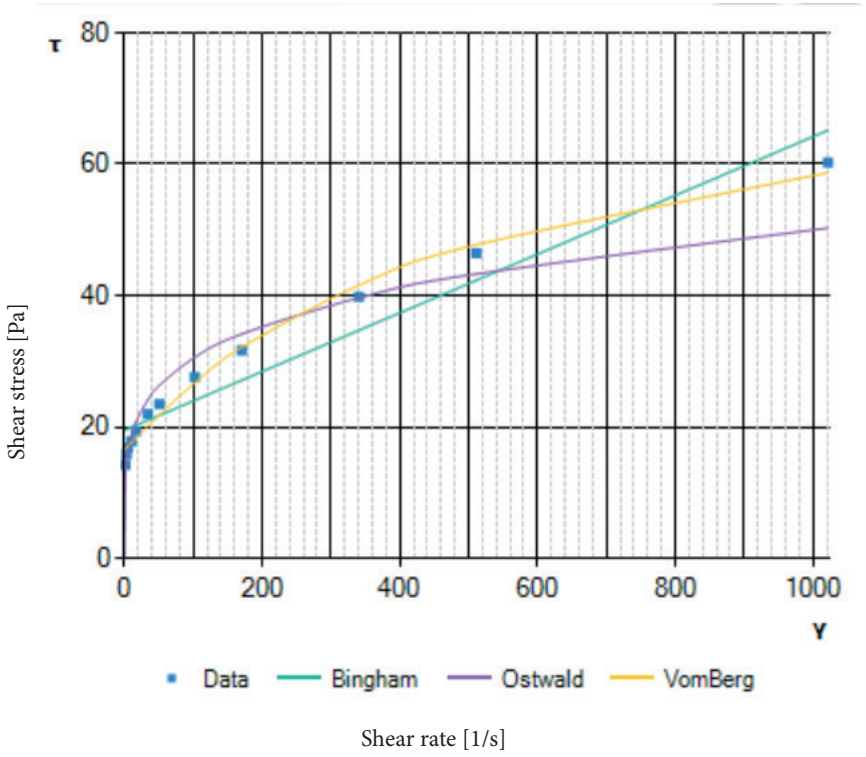

Fig. 8. Comparison of the Vom Berg model with the Bingham and Ostwald–de Waele model (API) for sample No. 8

Table 17. Results of rheological measurements for sample No. 9
(Bentonite 5% with the addition of 0.3% xanthan gum and Alcomer 0.02% + Desco 0.2% (BWOC))

Rotor speed [rot/min]	Angle [o]	Shear rate [1/s]	Shear stress [Pa]
600	92	1 022.040	46.982
300	67	511.020	34.215
200	55	340.680	28.087
100	42	170.340	21.448
60	36	102.204	18.384
30	29	51.102	14.810
20	26	34.068	13.278
10	22	17.034	11.235
6	20	10.220	10.214
3	17	5.110	8.682
2	16	3.406	8.171
1	15	1.703	7.660

Table 18. Summary of correlation coefficients of the analyzed rheological models for sample No. 9

Rheological model	Pearson correlation coefficient, R	Fischer–Sneadecor coefficient, F	Sum of squares, U
Bingham	0.969	157.452	98.03
Ostwald–de Waele	0.971	167.507	92.48
Vom Berg	0.992	599.254	26.94

Determined rheological parameters of the Vom Berg model for sample No. 9: parameter B = 12.19 Pa·s, parameter C = 110.302 [–], parameter YP = 8.301 Pa.

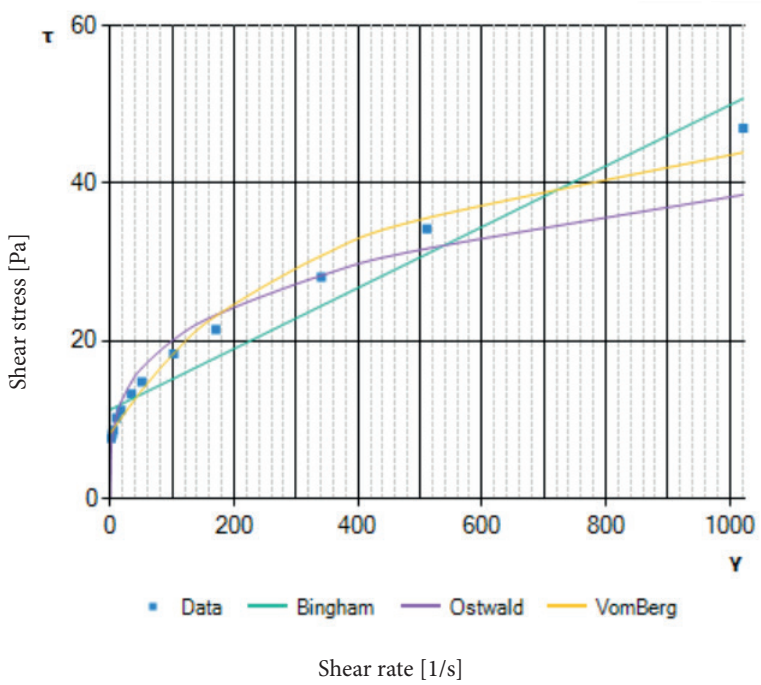

Fig. 9. Comparison of the Vom Berg model with the Bingham and Ostwald–de Waele model (API) for sample No. 9

Conclusions

The laboratory studies conducted at the Drilling Fluids Laboratory of the Faculty of Drilling, Oil, and Gas aimed to assess the applicability of the Vom Berg rheological model in describing the relationship between shear stress and shear rate in polymer-modified drilling muds. The results indicate that this model exhibits significantly higher correlation with experimental data compared to the Bingham and Ostwald–de Waele models, which are widely used in API methodology, particularly in the case of polymer-enhanced drilling muds. In the control sample, which consisted of a simple bentonite-based mud (5% Bentopol Zębiec bentonite) [15], the highest correlation was obtained for the Bingham model (R = 0.987), suggesting that in simple water-bentonite systems, its linear nature provides a better fit than the nonlinear Vom Berg model (R = 0.953). However, the situation changes with the introduction of polymer modifications. Upon adding 0.1% xanthan biopolymer in sample 2, the correlation coefficient for the Vom Berg model increased to 0.998, whereas for the Bingham model, it dropped to 0.973, and for the Ostwald–de Waele model, it was 0.944. In sample 6, where the biopolymer concentration was increased to 0.3%, this trend persisted – the Vom Berg model achieved a correlation of 0.994, outperforming both the Bingham model (0.972) and the Ostwald–de Waele model (0.961). The analysis of the remaining samples (3, 4, 5, 7, 8, and 9), which were further modified with Alcomer and Desco, confirmed the superior correlation of the Vom Berg model in describing their rheological behavior. Alcomer is widely used as a hydration inhibitor and filtration control agent, while Desco acts as a dispersant, improving viscosity control [12, 13]. The inclusion of these additives aimed to replicate real-world drilling fluid compositions, ensuring a more practical evaluation of the effectiveness of the tested rheological models.

The findings indicate that while API-recommended models, particularly the Bingham model, provide a good correlation (with coefficients not falling below 0.94), the Vom Berg model consistently exhibits a higher level of accuracy for polymer-modified drilling muds. The Ostwald–de Waele model, with correlation values not lower than 0.95, proves most effective in the low shear rate range, whereas the Bingham model, though more versatile across a wide range of shear rates encountered in drilling operations, does not fully capture the complex flow behavior of polymer-enhanced drilling muds.

The key conclusion of this study is that while API-recommended rheological models ensure a satisfactory fit to experimental data for laboratory-tested drilling muds, the application of the RheoSolution methodology and the use of the Vom Berg model significantly enhance the correlation, achieving values close to unity. These results suggest that the Vom Berg model may serve as a more appropriate tool for describing the rheology of polymer-modified drilling muds, offering potential benefits for improving the design and performance control of drilling fluids used in the oil and gas industry.

References

[1] American Petroleum Institute. *API Recommended Practice 13D: Rheology and Hydraulics of Oil-well Drilling Fluids*, 7th ed. Reaffirmed May 2023. API Publishing Services, Washington, D.C. 2023.
[2] Ferraris C.F.: *Measurement of the Rheological Properties of High Performance Concrete: State of the Art Report*. Journal of Research of the National Institute of Standards and Technology, 104, 5, 1999.
[3] Fann Instrument Company: *Model 35 Viscometer Instruction Manual*, 2013. www.fann.com [15.02.2025].
[4] Mendenhall W., Sincich T.: *A Second Course in Statistics: Regression Analysis*, 8th ed. Pearson Education, Inc. 2016.
[5] Rawlings J.O., Pentula S.G., Dickey D.A.: *Applied Regression Analysis: A Research Tool*, 2nd ed. Springer, New York 1998.
[6] Bingham E.C.: *Fluidity and Plasticity*. McGraw-Hill 1922.
[7] González R., Tamburrino A., Vacca A., Iervolino M.: *Pulsating Flow of an Ostwald–De Waele Fluid between Parallel Plates*. Water, 12, 4, 932, 2020. https://doi.org/10.3390/w12040932.
[8] Wiśniowski R., Skrzypaszek K., Toczek P.: *Selection of a Suitable Rheological Model for Drilling Fluid Using Applied Numerical Methods*. Energies, 13, 12, 3192, 2020.
[9] Wiśniowski R., Skrzypaszek K., Toczek P.: *Vom Berg and Hahn–Eyring Drilling Fluid Rheological Models*. Energies, 15, 5583, 2022. https://doi.org/10.3390/en15155583.
[10] Press W.H., Teukolsky S.A., Vetterling W.T., Flannery B.P.: *Numerical Recipes: The Art of Scientific Computing*, 3rd ed. Cambridge University Press 2007.
[11] Chapra S.C., Canale R.P.: *Numerical Methods for Engineers*, 7th ed. McGraw-Hill Education 2015.
[12] BASF SE: *Alcomer® Dewatering Agents for Drilling Fluids*. https://energy-resources.basf.com/global/en/oilfield-chemicals/applications/drilling/dewatering-agents [15.02.2025].
[13] Fann Instrument Company. *Model 35 Viscometer Instruction Manual*, 2013. www.fann.com [15.02.2025].
[14] Wiśniowski R., Stryczek S., Skrzypaszek K.: *Kierunki rozwoju badań nad reologią płynów wiertniczych*. Wiertnictwo, Nafta, Gaz, 24, 1, 2007, pp. 595–607.
[15] Zakłady Górniczo-Metalowe „Zębiec" S.A.: *Bentopol Zębiec – Bentonit do płuczek wiertniczych*. https://www.zebiec.pl/mineraly/wiertnictwo/bentopol-zebiec/ [15.02.2025].

Nomenclature

a, b, c – regression model coefficients [–]
B, C – rheological parameter in the Eyring model [–]
F – Fisher–Snedecor index [–]
U – sum of squared residuals [–]
dv/dr – shear rate gradient [s^{-1}]
η_{pl} – plastic viscosity [Pa·s]
$\dot{\gamma}_I$ – shear rate measured at i-th rotational speed [s^{-1}]
k – coefficient of consistency [Pa·s^n]
m – number of measurements with viscometer [–]
n – exponential index [–]
R – Pearson's correlation coefficient [–]
τ – shear stress [Pa]
τ_i – shear stress measured at i-th rotational speed [Pa]
YP, τ_y – yield point [Pa]
$\bar{\tau}$ – average value of shear stress [Pa]

Journal of Geotechnology and Energy | vol. 42 | no. 1 | 2025 | pp. 21–26

https://doi.org/10.7494/jge.2025.42.1.7007

ARTICLE

AN ECONOMIC ANALYSIS MODEL FOR LITHIUM PRODUCTION BY DIRECT LITHIUM EXTRACTION (DLE) METHOD FROM A SINGLE WELL

Adam Jan Zwierzyński

AGH University of Krakow, Faculty of Drilling, Oil and Gas, Poland
ORCID: 0000-0002-2568-6446
e-mail: zwierzyn@agh.edu.pl

Date of submission:
13.02.2025

Date of acceptance:
27.02.2025

Date of publication:
31.03.2025

https://journals.agh.edu.pl/jge

Abstract: The article presents an economic model enabling the assessment of the profitability of lithium extraction using the direct lithium extraction (DLE) method from geothermal brines from a single well. The model enables a preliminary simplified assessment of the profitability of DLE projects, which can be helpful in selecting the optimal locations for such projects and drilling production wells. The article also presents the critical role of lithium as a raw material for the decarbonization of the global economy, methods of its extraction, and the economic prospects of the market for this raw material. It also presents exemplary DLE projects in the world.

Keywords: lithium, brine, lithium geothermal brine, lithium direct extraction, LDE

1. Lithium as a critical raw material for energy transformation

Lithium is one of the critical materials in terms of the world's energy transformation towards climate-neutral economies as it is a raw material necessary for the production of batteries. The European Commission has listed lithium as one of 34 critical raw materials for its development [1]. Battery production is not only needed for the development of electromobility, but also for industrial energy storage, which is necessary for the further development and wider use of renewable energy sources in the energy sector. Unfortunately, in the case of industrial energy storage, their costs are still so high that they are of limited use in large energy applications. The currently dominant battery technology on the market is lithium-ion (Li-ion) batteries, which have gained great popularity in consumer and industrial applications. In turn, battery technologies are mainly used for the production of energy storage:

- lithium-ion (Li-ion) – the most popular technology today;
- lithium-iron-phosphate (LFP);
- lithium-nickel-cobalt-aluminum-oxide (NCA);
- lithium-manganese (LMO);
- lithium-cobalt (LCO);
- lithium-titanium (LTO).

The listed battery technologies use lithium as one of the main components. The value of the global lithium market [2] is estimated at about $9.86 billion (2024). It is estimated that by 2033 the global lithium market will increase several times and reach $28.45 billion. This means that from 2024 to 2033 the CAGR for the lithium market will be 12.50%. Lithium metal [2] is used in metallurgy (refining iron, nickel, copper and zinc). Lithium [2] is also used in the chemical industry for organic synthesis. For example, the reagent, n-butyl lithium, is one of the main initiators of polymerization processes in the production of synthetic rubber. Lithium is also [2] used in the pharmaceutical industry. Lithium metal is also an important element of various battery technologies. It is used as an anode in lithium batteries due to its low mass and high negative electrochemical potential. As mentioned earlier, the use of lithium in battery production makes it a key raw material for the success of the energy transformation.

The report [2] also presents forecasts for markets strongly linked to lithium production, whose products require this raw material for their production:

- lithium-ion Battery Recycling Global Market: USD 8.10 billion (2023), USD 10.26 billion (2024). Forecast: USD ~85.69 billion by 2033, CAGR of 26.6% from 2024 to 2033;
- lithium Iron Phosphate Battery Global Market: USD 12.7 billion (2022). Forecast: USD ~54.36 billion by 2032 with CAGR of 15.7%;
- lithium Titanate Batteries Global Market: USD 56 billion (2022). Forecast USD ~185.93 billion (2032) with CAGR of 12.8%;
- Fiber Batteries Global Market: USD 83.90 million (2023). Forecast: USD ~386.55 million (2032) with CAGR of 18.50%;
- Action Camera Global Market: USD 2.8 billion (2023). Forecast: USD ~6.39 billion (2033) with CAGR of 8.6% from 2024 to 2033;
- Industrial Batteries Global Market: USD 42.04 billion (2023). Forecast: USD 463.63 billion (2033) with CAGR of 27.02% from 2024 to 2033.

The countries that dominate lithium production [3] are China and Australia. China not only extracts lithium but also processes it into other products. Australia, on the other hand, mainly extracts lithium as a raw material and sells it on international markets. The fact that most of the supplies of raw materials (including lithium) recognized by the European Commission as critical for the development of the EU economy come from outside the EU was one of the reasons for the adoption on April 11, 2024 of Regulation 2024/1252 on critical raw materials (the so-called Critical Raw Materials Act), which assumes that by 2030:

- the extraction capacity of critical raw materials in the EU is to cover at least 10% of the annual consumption of strategic raw materials in the EU;
- the processing capacity of critical raw materials in the EU should be at least 40%;
- the recycling capacity of critical raw materials in the EU should be at least 15%.

In the case of lithium, this means that the EU and its member states will take a number of actions to increase lithium production within the EU and become independent from supplies from outside the EU.

Providing stable and cheap sources of lithium is also important for the development of the Polish economy. Poland is the second largest global producer of lithium-ion batteries for the electromobility sector. Paper [4] presents the location of projects from the electromobility sector in Poland divided into individual segments – production of batteries and components for them, production of electric vehicles, production of e-buses and centers for the development of EV-related technologies. In addition to LG Energy Solutions, other leading companies (e.g. Northvolt, Umicore, SK Innovation, Capchem, Guotai Huarong, BMZ, Mercedes-Benz Manufacturing Poland) from the battery sector are also investing in Poland.

In 2021, 540,000 tons of lithium were produced worldwide and according to the predictions of the World Economic Forum, by 2030 this number will have to increase to over 3 million tones. The demand for lithium may increase up to 8-fold by 2040 and 10-fold by 2050 – according to the forecasts of the International Energy Agency. The world could face a lithium shortage as early as 2025. According to BMI (one of the research units of the Fitch Solutions organization), this state of affairs will be mainly responsible for the high demand for this element in China, which will significantly exceed the supply. According [5] to a report published by BMI researchers, China's demand for lithium for electric vehicles will grow by approximately 20.4% each year from 2023 to 2032. However, at the same time, the supply of this element in China will increase only by 6%. BMI clearly states in its report that this percentage cannot cover even 1/3 of China's total lithium demand. Global lithium demand forecast divided into various industries was presented in paper [6].

2. Lithium production from geothermal brine

There are three main sources of lithium and methods of its production. The first method involves obtaining it from hard rocks, spodumene, and sedimentary rocks. This is an expensive method, requiring the construction of an open-pit mine and large investment outlays. Such an investment requires a large area of land, fulfilling many formalities and obtaining many permits, and it is also energy-intensive. The lithium produced is unlikely to be climate neutral – it depends on whether the energy supplying such a mine and the devices operating in it comes from zero-emission sources and whether the fleet of mining trucks has been fully electrified. Another method involves obtaining lithium from brines, which are stored in tanks for the natural evaporation (under the influence of the sun and temperature) of water from them. Both methods are not ecological and require a large area for their implementation, which is taken from nature or residents for the duration of lithium exploitation, and then it should be reclaimed, which means additional costs.

There is a third method, which is much more ecological and is considered the future of the lithium mining industry. It involves direct extraction of lithium from geothermal brines, which are extracted from the rock mass by drilling holes. The brine is first extracted to the surface using exploitation holes, in a special Direct Lithium Extraction (DLE) installation (lithium is recovered from it), and then it is re-injected into the rock mass using injection holes. The brine circulates in a closed circuit and is not released into the environment. If the entire installation is powered by electricity from renewable energy sources (RES), the lithium produced will be climate neutral. Such an investment does not require a large area for its operation. It only needs:

- spaces for production heads;
- spaces for injection heads;
- spaces for Direct Lithium Extraction (DLE) installations;
- possibilities of running pipelines connecting the above elements.

This investment is also much less cost-intensive than the two previous methods and, unlike them, has only a minimal impact on the natural environment.

There are already some companies in the world that are already involved in the extraction of lithium using the DLE method. One of the most famous places in the world where DLE projects are being developed is the Salton Sea in California, USA. This region is called Lithium Valley and various energy companies are investing in this area. The waters in this area are highly saline and rich in minerals. The lake is located on the San Andreas fault line and has a high amount of geothermal heat. Geothermal energy projects have been developed in this area for many years. In recent years, companies have attempted to extract mineral resources from the geothermal brine. It is estimated that the aquifers near the Salton Sea may contain enough lithium to meet almost 40% of the world's lithium demand. Using DLE technologies, some companies are now extracting lithium from the brine and recovering geothermal energy. Previously, lithium-rich brine was only a byproduct of geothermal energy production and the lithium in it was not exploited.

Europe also has deposits of lithium-rich brines. The publication [7] presents the results of the EuGeLi project, in which the well data for Western Europe were analyzed for the occurrence of lithium-rich brines. Four highly prospective areas in Western Europe were identified. It should be emphasized that the study did not perform analyses for the countries of Central and Eastern Europe.

In Poland, there are also areas containing deposits of geothermal brines rich in lithium [8] with concentrations reaching even above 200 mg/L. However, the Polish potential of geothermal brines containing lithium is still largely unmapped and requires extensive research.

DLE projects are no longer just academic considerations tested in laboratories. Such projects are already being implemented in various parts of the world and

are being invested in by serious small and large investors. This is demonstrated by the four examples presented below.

Among the most well-known projects for lithium extraction from brines is the project in the Upper Rhine Valley, carried out by Vulcan Energy Resources Ltd, which is in the development phase. Vulcan has granted 16 licenses in the Upper Rhine Valley, for a total secured concession area of 1,790 km^2. Vulcan market capitalization is AUD 900 million (4 February 2025). Vulcan's [9] potential resources are 27.7 tones of LCE (Lithium Carbon Equivalent). Major investors are:

- stellantis corporation (5%);
- Hancok Prospecting Pty Ltd (6%);
- CIMIC Group (6%).

Another well-known DLE project is the project located 25 miles west of the town of Magnolia in southwestern Arkansas, owned by Standard Lithium Ltd. [10] with 1.4/0.4 million tones LCE (Lithium Carbon Equivalent). Estimated Indicated/Inferred Resource. The company has drilled over 400 boreholes and has planned +30,000 tons lithium hydroxide annual production which after conversion to LCE (by multiplying the conversion factor 0.88) is +26,400 tones of LCE. Company market capitalization is CAD 388.87 million (4 February 2025). Lithium avg. Grade of 437 mg/L. Equinor has joined Standard Lithium Ltd investors as a strategic partner.

Another DLE project is project Prairie Lithium Project owned by Arizona Lithium Ltd. with license area 390,000 acres, the size of the deposit estimated at 6.3 million tones LCE, depth 2.4 km, the thickness of the formation 140 m and lithium concentration 101–106 mg/L. Technical and economic feasibility study was presented in publication [11]. The Prairie project estimated at 4.1 million tones LCE was acquired by Arizona Lithium Ltd in December 2022 for CAD 70.6 million, where CAD 40 million was in cash.

In 2023, the private company Galvanic Energy sold licenses with an area of 120,000 acres in the Smackover geological formation rich in geothermal brine containing lithium with an estimated volume of 4 million tones LCE to ExxonMobil for an amount of over USD 100 million.

3. DLE well economic analysis – methods

In planning DLE projects, it is important to conduct an economic analysis for a single production well, as well as for the entire project. There are many factors that need to be taken into account, such as the cost of geological surveys, purchase or lease of the DLE installation, and drilling boreholes. Demand and possible price development scenarios should also be analyzed. One of the most expensive investment phases (apart from purchasing the DLE installation) is drilling boreholes. Therefore, this part of the economic analysis of DLE projects was focused on. An analysis was performed for an example geothermal brine deposit with a lithium concentration of 217 ppm located at a depth of 2 km. In order to be able to exploit such a deposit, it is necessary to drill a production hole 2,000 m deep. The average cost of drilling 1 meter of a hole in Poland is 10,000 PLN/m, which means that the hole will cost PLN 20 million, or about USD 5 million. There is a risk that despite promising lithium concentrations, the obtained brine flows may be too small. On the other hand, brine flows may be large, but the lithium concentration may be lower than assumed. It is necessary to analyze the profitability of a single borehole depending on the obtained brine flows and lithium concentrations in it. The annual lithium production from a single borehole is described by formula (1). For this purpose, the brine flow rate [l/s] should be multiplied by 3,600 (this is the number of seconds in 1 hour) and then multiplied by 24 hours. It is unlikely that DLE installations will operate 365 days a year, because such installations will usually require at least several days for service operations. Here, it was assumed that the number of operating days U will be 358, i.e. the total interruption in DLE operation will be 7 days, which seems to be a reasonable assumption. SE is the effective concentration, which is calculated by converting the concentration in parts per million to the concentration in mg/L and multiplying it by the lithium capture efficiency factor of the DLE installation, which is assumed to be 0.75 (i.e. 75%). In reality, the lithium capture efficiency of DLE installations can be much higher and exceed 90%, but it depends on the type of installation, the sorbent used, and the composition of the brine. The factor 10^{-9} is used to convert units expressed in milligram to tons. The last factor 5.323 is used to calculate lithium carbon equivalent (LCE). In the industry, lithium is sold in the form of several types of its compounds, which contain different concentrations of it. For standardization, lithium carbon equivalent (LCE) is used for billing and comparing lithium projects. In our case, we produce pure lithium. The factor 5.323 is used to convert the mass of pure lithium to the mass of lithium carbonate corresponding to the same amount of lithium. Figure 1 presents the calculated results of annual LCE production depending on the brine flow rate [l/s] and lithium concentration [ppm].

The annual incomings before tax are determined based on formula (2), which is a slight modification of formula (1). If the annual production obtained using formula (1) is multiplied by P, which is the market price of lithium (USD/tLCE), the annual pre-tax revenue from one well is obtained. This is expressed by formula (2). Since the analysis was originally performed at the turn of spring and summer 2024, the price from that period was assumed to be P = 14,800 USD/tLCE. There is one problem here that has not been taken into account. The DLE installation consumes energy and its operating cost is not zero. This can be taken into account in formula (3) by using as P the value of the market price USD/tLCE from which the cost of obtaining 1 ton of LCE has been subtracted. In the analyzed one, an updated value of P was assumed of 10,000 tLCE. After its substitution in formula (3), instead of annual income before taxation, the profit before taxation is obtained. Figure 2 shows the annual profit from one well depending on the brine inflow rate [l/s] and lithium concentration [ppm].

$$LCE\ Production = \\ = F \cdot 3600 \cdot 24 \cdot U \cdot SE \cdot 10^{-9} \cdot 5.323 \tag{1}$$

$$Income\ before\ tax = \\ = F \cdot 3600 \cdot 24 \cdot U \cdot SE \cdot 10^{-9} \cdot P \cdot 5.323 \tag{2}$$

where:

3,600 – number of seconds in 1 hour,
24 – number of hours during day,
F – flow rate [l/s],
U – the number of days a year the installation operates (U = 358),
SE – effective concentration (concentration ppm converted to mg/l using the DLE system conversion factor = 0.75),
10^{-9} – 1 mg is 10^{-9} tones,
P – market price per ton of LCE.

		PRODUCTION tons LCE/year											
		Concentration ppm											
		25	50	75	100	125	150	175	200	225	250	275	300
F (Flow Rate) l/s	5	15.44	30.87	46.31	61.74	77.18	92.61	108.05	123.49	138.92	154.36	169.79	185.23
	10	30.87	61.74	92.61	123.49	154.36	185.23	216.10	246.97	277.84	308.71	339.58	370.46
	15	46.31	92.61	138.92	185.23	231.53	277.84	324.15	370.46	416.76	463.07	509.38	555.68
	20	46.31	92.61	138.92	185.23	231.53	277.84	324.15	370.46	416.76	463.07	509.38	555.68
	25	77.18	154.36	231.53	308.71	385.89	463.07	540.25	617.43	694.60	771.78	848.96	926.14
	30	92.61	185.23	277.84	370.46	463.07	555.68	648.30	740.91	833.52	926.14	1,018.75	1,111.37
	35	108.05	216.10	324.15	432.20	540.25	648.30	756.35	864.40	972.45	1,080.49	1,188.54	1,296.59
	40	123.49	246.97	370.46	493.94	617.43	740.91	864.40	987.88	1,111.37	1,234.85	1,358.34	1,481.82
	45	138.92	277.84	416.76	555.68	694.60	833.52	972.45	1,111.37	1,250.29	1,389.21	1,528.13	1,667.05
	50	154.36	308.71	463.07	617.43	771.78	926.14	1,080.49	1,234.85	1,389.21	1,543.56	1,697.92	1,852.28
	55	169.79	339.58	509.38	679.17	848.96	1,018.75	1,188.54	1,358.34	1,528.13	1,697.92	1,867.71	2,037.50
	60	185.23	370.46	555.68	740.91	926.14	1,111.37	1,296.59	1,481.82	1,667.05	1,852.28	2,037.50	2,222.73
	65	200.66	401.33	601.99	802.65	1,003.32	1,203.98	1,404.64	1,605.31	1,805.97	2,006.63	2,207.30	2,407.96
	70	216.10	432.20	648.30	864.40	1,080.49	1,296.59	1,512.69	1,728.79	1,944.89	2,160.99	2,377.09	2,593.19
	75	231.53	463.07	694.60	926.14	1,157.67	1,389.21	1,620.74	1,852.28	2,083.81	2,315.35	2,546.88	2,778.41
	80	246.97	493.94	740.91	987.88	1,234.85	1,481.82	1,728.79	1,975.76	2,222.73	2,469.70	2,716.67	2,963.64
	85	262.41	524.81	787.22	1,049.62	1,312.03	1,574.43	1,836.84	2,099.25	2,361.65	2,624.06	2,886.46	3,148.87
	90	277.84	555.68	833.52	1,111.37	1,389.21	1,667.05	1,944.89	2,222.73	2,500.57	2,778.41	3,056.26	3,334.10
	95	293.28	586.55	879.83	1,173.11	1,466.39	1,759.66	2,052.94	2,346.22	2,639.49	2,932.77	3,226.05	3,519.32
	100	308.71	617.43	926.14	1,234.85	1,543.56	1,852.28	2,160.99	2,469.70	2,778.41	3,087.13	3,395.84	3,704.55

Fig. 1. Annual production of LCE by one borehole

		PROFIT in millions US$ annually											
		Concentration ppm											
		25	50	75	100	125	150	175	200	225	250	275	300
F (Flow Rate) l/s	5	0.15	0.31	0.46	0.62	0.77	0.93	1.08	1.23	1.39	1.54	1.70	1.85
	10	0.31	0.62	0.93	1.23	1.54	1.85	2.16	2.47	2.78	3.09	3.40	3.70
	15	0.46	0.93	1.39	1.85	2.32	2.78	3.24	3.70	4.17	4.63	5.09	5.56
	20	0.62	1.23	1.85	2.47	3.09	3.70	4.32	4.94	5.56	6.17	6.79	7.41
	25	0.77	1.54	2.32	3.09	3.86	4.63	5.40	6.17	6.95	7.72	8.49	9.26
	30	0.93	1.85	2.78	3.70	4.63	5.56	6.48	7.41	8.34	9.26	10.19	11.11
	35	1.08	2.16	3.24	4.32	5.40	6.48	7.56	8.64	9.72	10.80	11.89	12.97
	40	1.23	2.47	3.70	4.94	6.17	7.41	8.64	9.88	11.11	12.35	13.58	14.82
	45	1.39	2.78	4.17	5.56	6.95	8.34	9.72	11.11	12.50	13.89	15.28	16.67
	50	1.54	3.09	4.63	6.17	7.72	9.26	10.80	12.35	13.89	15.44	16.98	18.52
	55	1.70	3.40	5.09	6.79	8.49	10.19	11.89	13.58	15.28	16.98	18.68	20.38
	60	1.85	3.70	5.56	7.41	9.26	11.11	12.97	14.82	16.67	18.52	20.38	22.23
	65	2.01	4.01	6.02	8.03	10.03	12.04	14.05	16.05	18.06	20.07	22.07	24.08
	70	2.16	4.32	6.48	8.64	10.80	12.97	15.13	17.29	19.45	21.61	23.77	25.93
	75	2.32	4.63	6.95	9.26	11.58	13.89	16.21	18.52	20.84	23.15	25.47	27.78
	80	2.47	4.94	7.41	9.88	12.35	14.82	17.29	19.76	22.23	24.70	27.17	29.64
	85	2.62	5.25	7.87	10.50	13.12	15.74	18.37	20.99	23.62	26.24	28.86	31.49
	90	2.78	5.56	8.34	11.11	13.89	16.67	19.45	22.23	25.01	27.78	30.56	33.34
	95	2.93	5.87	8.80	11.73	14.66	17.60	20.53	23.46	26.39	29.33	32.26	35.19
	100	3.09	6.17	9.26	12.35	15.44	18.52	21.61	24.70	27.78	30.87	33.96	37.05

Payback time for the cost of drilling a borehole in years (cost of drilling a hole 5.01 million US$)

≤ 0.5	≤ 1	≤ 2	≤ 3	> 3

Fig. 2. Annual incomings from one borehole at assumed market price 14,800 USD/tLCE

4. Discussion

The economic model created is very simplified and certain technological and economic assumptions have been made in it. The model ignores the fact that an injection well must also be made in addition to the production well if the brine is to circulate in a closed circuit. It may also be necessary to make more and more complex holes than a simple vertical hole. There are at least several companies in the world that produce and sell DLE installations. However, the selection of the appropriate installation will significantly affect the economics of the project – starting with the efficiency of lithium extraction, the costs of lithium extraction, and ending with the cost of the installation itself. There are large stationary DLE installations (e.g. Sunresin), which resemble small production plants, their cost is high and the construction time is long. There are also small modular mobile installations (DLE) (e.g. International Battery Metals – up to 95% recovery rate), the cost of which is much lower and can be leased. Choosing leasing instead of purchasing a DLE installation can reduce the initial investment required to start production. This is not taken into account in the economic model. It also uses outdated lithium market prices (14,800 USD/tones of LCE) from the period at the turn of spring/summer 2024 when the presented modeling was conducted. Currently, the market price of lithium (USD/tones of LCE) is around 10,829 USD/tones of LCE. The model also does not take into account the cost of geological work to extract and recognize lithium-rich brine deposits, which may be significant. It is worth adding that the brine may contain other valuable elements, and it is also possible to recover heat from it, which further improves the economics of the project.

Despite many simplifications, the presented economic model provides a lot of valuable information. It shows that there is a large margin (lithium concentration [ppm], brine flow rate [l/s]) for which a single well should pay off. Analysis of the data in Figure 2 shows that the well will not pay off in less than 3 years only for extremely unfavorable cases. These data are a strong argument reducing the risk for a potential investor. Given good geological conditions and promising lithium concentrations in the brine, the well would have to be drilled very incorrectly to make it unprofitable and its cost would not be recovered within a few years.

5. Conclusions

Lithium is a critical raw material on which the success of the energy transformation depends. According to the data presented in the article, the lithium market is very promising and is a strongly growing market, which may experience a supply gap in the future. Unfortunately, the need to obtain lithium, e.g. for the production of batteries, is criticized by ecologists due to the previously used non-ecological methods of its extraction, which have had a negative impact on the natural environment. However, it is possible that in the future lithium will be obtained using ecological methods using the Direct Lithium Extraction (DLE) method from geothermal brines. There are already companies in the world that implement such projects on a large scale, as well as companies producing and selling DLE installations. The economic modeling carried out in the article shows that such projects are highly profitable. Unfortunately, there is a lack of data in Poland to be able to select the most promising regions where geothermal brines rich in lithium occur. Lithium is also an important raw material for Poland, which is the world's second largest producer of lithium-ion batteries, and electromobility in the country is developing.

Funding: This research received no external funding.

Acknowledgments: Special thanks to Geolithium PSA.

References

[1] Regulation of the European Parliament and of the Council. Establishing a framework for ensuring a secure and sustainable supply of critical raw materials and amending Regulations (EU) 168/2013, (EU) 2018/858, 2018/1724 and (EU) 2019/1020, Annex II, Section 1 – List of critical raw materials. https://eur-lex.europa.eu/legal-content/EN/TXT/?uri=CELEX%3A52023PC0160 [4.02.2025].

[2] *Lithium Market Size Expected to Achieve USD 28.45 Billion by 2033*. https://www.globenewswire.com/news-release/2024/09/10/2944010/0/en/Lithium-Market-Size-Expected-to-Achieve-USD-28-45-Billion-by-2033.html [4.02.2025]

[3] European Commission: Directorate-General for Internal Market, Industry, Entrepreneurship and SMEs, Grohol, M. and Veeh, C.: *Study on the critical raw materials for the EU 2023 – Final report*. Publications Office of the European Union, 2023, https://data.europa.eu/doi/10.2873/725585 [4.02.2025].

[4] Industry report „*Elektromobilność w Polsce: Inwestycje, Trendy, Zatrudnienie*", Polish Investment and Trade Agency in cooperation with Bergman Engineering and Polish Chamber of Electromobility Development. https://www.paih.gov.pl/wp-content/uploads/0/144601/144608.pdf [4.02.2025].
[5] *BMI Predicts Lithium Shortfall in 2025.* https://www.miningnewswire.com/bmi-predicts-lithium-shortfall-in-2025/ [4.02.2025].
[6] Lu S., Frith J.: *Will the Real Lithium Demand Please Stand Up? Challenging the 1Mt-by-2025 Orthodoxy*. BloombergNEF, 2019. https://about.bnef.com/blog/will-the-real-lithium-demand-please-stand-up-challenging-the-1mt-by-2025-orthodoxy/ [4.02.2025].
[7] Sanjuan B., Gourcerol B., Millot R., Rettenmaier D., Jeandel E., Rombaut A.: *Lithium-rich geothermal brines in Europe: An up-date about geochemical characteristics and implications for potential Li resources*. Geothermics, 101, pp. 102385, 2022. https://doi.org/10.1016/j.geothermics.2022.102385.
[8] Razowska-Jaworek L., Pasternak M.: *Potential lithium resources in geothermal brines and saline mine waters in Poland (poster)*. Lithium Symposium, Vienna, Austria 2024. http://doi.org/10.13140/RG.2.2.26371.82728.
[9] *Vulcan Energy Corporate Presentation Q1 2025*. https://api.investi.com.au/api/announcements/vul/bc4408d4-408.pdf [4.02.2025].
[10] *Standard Lithium January 2025 Management Presentation*. https://www.standardlithium.com/investors/company-information/presentations [4.02.2025].
[11] Arizona Lithium. https://www.arizonalithium.com/wp-content/uploads/2024/01/02758730.pdf [4.02.2025].

Journal of Geotechnology and Energy | vol. 42 | no. 1 | 2025 | pp. 21–26

https://doi.org/10.7494/jge.2025.42.1.6754

ARTICLE

AN ANALYSIS OF HYDROGEN GAS SATURATION IN THE SEDIMENTARY SEQUENCES OF VOLYN-PODILLYA (UKRAINE)

Ihor Hubych

Ivan Franko National University of Lviv, Ukraine
ORCID: 0000-0002-6812-2974
e-mail: ihor.hubych@lnu.edu.ua

Yurii Krupskyi

Ivan Franko National University of Lviv, Ukraine
ORCID: 0000-0002-2282-3310
e-mail: iurii.krupskyi@lnu.edu.ua

Serhii Tsikhon

Ivan Franko National University of Lviv, Ukraine
ORCID: 0000-0003-3423-5767
e-mail: serhii.tsikhon@lnu.edu.ua

Date of submission:
21.11.2024

Date of acceptance:
9.01.2025

Date of publication:
31.03.2025

https://journals.agh.edu.pl/jge

Abstract: With the aim of Ukrainian industry using hydrogen energy, the paper considers the general patterns of hydrogen distribution in the sedimentary sequences of Volyn-Podillya. The general features of the distribution of water-dissolved and sorbed gases in rocks within productive and water-saturated complexes are analyzed. The genetic relationships between individual components of natural gases have been established, which allows us to identify depth intervals where hydrogen predominates in the well section. The latter, when used for regional forecasting, makes it possible to establish zones, and thus directions for the search for hydrogen accumulations in the sedimentary cover in Volyn-Podillya.

Keywords: hydrogen, gases, forecast, core, fluid, well

1. Introduction

The interest in hydrogen energy is primarily driven by the fact that hydrogen is the most abundant element on the Earth's surface and in space, it holds the highest energy content, and its combustion produces only water and not carbon dioxide emissions. Industries are therefore investing heavily in hydrogen as a key component of the fight against climate change, as natural hydrogen, or "white hydrogen", is considered to be one of the cleanest fuels.

In the Lorraine region, near the French-German border, a group of scientists has recently made a revolutionary discovery in the earth's interior. Jacques Pironon, a professor at the University of Lorraine, believes that they have discovered one of the world's largest deposits of natural hydrogen. They were amazed with their find: *large bubbles of hydrogen gas in the water column* indicating a potentially huge natural hydrogen deposit [1].

Currently, Canada is the leader in the pure hydrogen production. At the same time, Japan is actively implementing and developing hydrogen technologies, and has even created a hydrogen "ministry" to completely switch from nuclear to hydrogen energy by 2050 [2].

Ukraine also has plans to use hydrogen. Currently, the lifetime of some Ukrainian nuclear power plants has been extended for the second time, and it is physically dangerous to do so for a third. The country is facing the issue of how to replace the generating capacities lost with these power plants being decommissioned, as NPPs account for 35% of Ukraine's energy balance [3].

2. Gas-geochemical properties of sedimentary sequences

In order for the industry to switch to hydrogen energy, it is necessary to study the patterns of hydrogen distribution in the sedimentary stratum. To this end, the paper analyzes the patterns of distribution of water-dissolved and rock-sorbed gases within productive and water-saturated bodies. The genetic relationships between individual components of natural gases have been established, which make it possible to distinguish depth ranges in the well section with a predominance of a certain type of gases, namely syn- or epigenetic hydrocarbon components, nitrogen, hydrogen and unsaturated hydrocarbons.

The specifics of hydrogeochemical criteria related to oil and gas content are based on the study of the patterns of distribution and migration of water-dissolved gases in sedimentary strata.

It should be noted that against the general regional background of nitrogen gases, there are areas with increased concentrations of hydrocarbon components and gas saturation of formation waters, which are confined to the contour zones of oil and gas deposits.

With the distance from the contour, the gas saturation of water and the hydrocarbon content in gases decrease, which is confirmed by actual data from many oil and gas regions. For example, in the Volga-Ural oil and gas region, according to L. Zorkin [4], clearing off the oil and gas contour, the gas saturation of water and the concentration of hydrocarbons in water-dissolved gases decrease while the nitrogen content increases (Fig. 1).

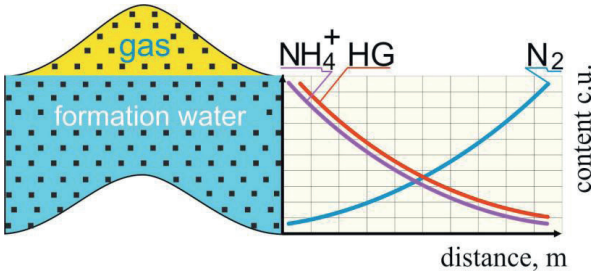

Fig. 1. Diagram of changes in hydrochemical parameters of formation water clear off the hydrocarbon reservoir contour
HG – hydrocarbon gases C_1-C_6 [%]; N_2 – nitrogen [%];
NH_4^+ – ammonium [mg/l];
content c.u. – conventional units

A similar pattern was detected by M. Gatalsky [5] in the Pripyat Basin, and by L. Shvay [6] in different stratigraphic horizons of the Dnipro-Donetsk Basin. The above shows that the main component of water-dissolved gases in different regions is nitrogen, and the presence of hydrocarbon gases is caused by the dispersion of hydrocarbons from deposits due to their diffusion in reservoir fluids.

If nitrogen is the main component of water-dissolved gases away from the hydrocarbon accumulation, the question arises regarding the reason why its content in formation water decreases as it approaches the reservoir contour. This is probably due to the transition of free nitrogen to the bound state in the form of ammonium (NH_4^+), the content of which is much higher in productive areas compared to water-saturated sections.

In the formation waters of prospective sites, ammonium and nitrogen demonstrate an inverse distribution, i.e. clear off the near-contour zone the ammonium concentration decreases while the nitrogen concentration increases (Fig. 1). For example, in the Crimean oil and gas region, the ratio of ammonium

to nitrogen (NH_4^+/N_2) in the near-contour waters of deposits is greater than 1, while it always decreases off the deposits [7].

The relationship between the forms of nitrogen NH_4^+ and N_2 is given in the work of J. Hunt [8], where it is expressed by the following equation (1):

$$N_2 + 3H_2 \leftrightarrow 2\,NH_3 + \Delta T \quad (1)$$

This process is in equilibrium and occurs in the gas phase with heat generation (ΔT); with a decrease in the temperature of the medium, the equilibrium shifts towards the evolution of ammonia, but the reaction rate slows down. Clay minerals containing aluminium oxide (Al_2O_3) can serve as a catalyst in formation conditions. The dissolution of ammonia in formation water and its removal as a reaction product facilitate the reaction.

Hydrogen is an important participant in the hydrochemical processes under consideration. There is no consensus on the sources of its origin and role in oil and gas origination. However, hydrogen is not only found in volcanic and metamorphic rocks, but also in sedimentary cover deposits; the latter, according to many researchers, is due to the catabolism of organic matter (OM).

3. Analysis of hydrogen distribution in geological sequences

Hydrogen is hardly ever found in the gases of oil and gas fields although there are a few exceptions. For example, one well is known in the Chechen Republic (Grozny district) and one in Uzbekistan, where the hydrogen content is 8.3 and 12.7%, respectively.

Hydrogen is also present in associated gases in a number of wells in Pennsylvania and Pittsburgh (USA), where its content reaches 7–35%. However, it should be noted that hydrogen is much more commonly present in a water-dissolved form in the formation waters of sedimentary basins [7].

V. Havrysh [9] believes that prolonged migration of hydrogen through the pore space leads to the origination of its own hydrodynamic systems, in which its oxidation processes occur in parallel with water exceedance, which causes leaching of rocks and brittle deformation development. This suggests that if the hydrogen content in the section is high, the latter will be water- or gas-saturated. For instance, in the Lokachynska-3 well, where the Middle Devonian rocks demonstrate high hydrogen content, a gas-water mixture was obtained during testing (Fig. 2).

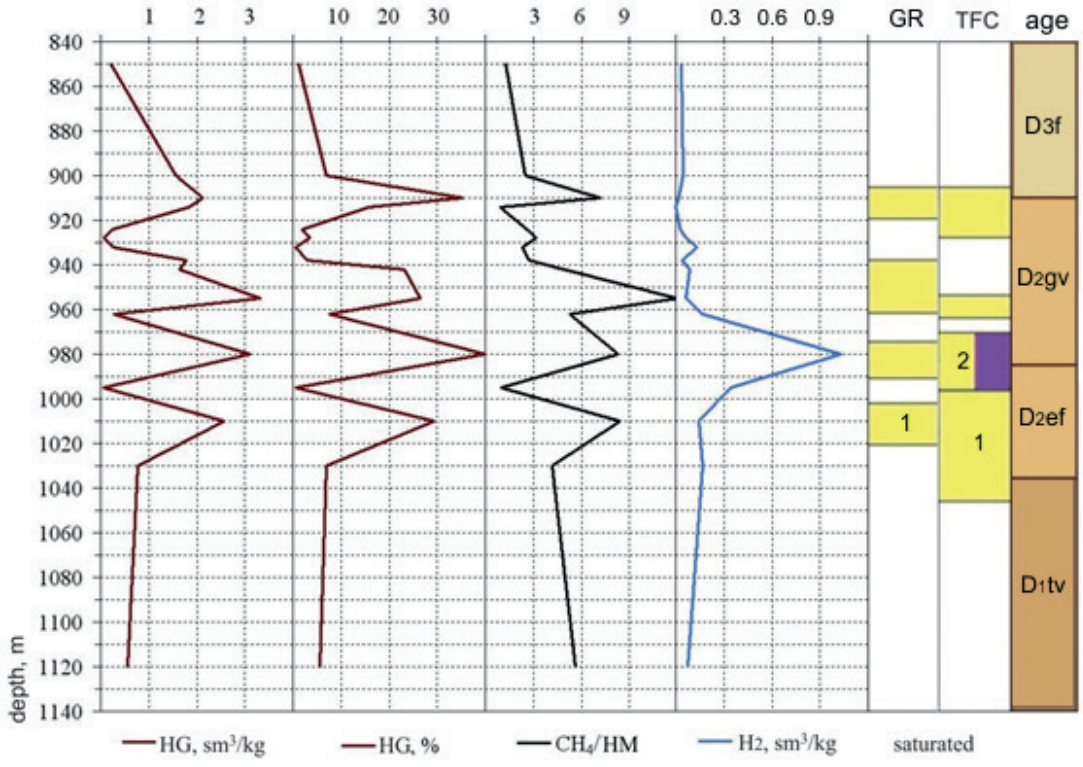

Fig. 2. Distribution of gas metering parameters in Lokachynska-3 well. HG – hydrocarbon gases C_1-C_6; H_2 – hydrogen; CH_4/HM – methane to homologues; GR – geochemical research, TFC – testing of formations in the column. Saturation: 1 – gas-saturated, 2 – water and gas saturated D_3fr – Frasnian; D_2gv – Givetian; D_2ef – Eifelian; D_1tv – Tiverska Series

It is also worth noting that unsaturated hydrocarbons (UH), such as ethylene (C_2H_4) and propylene (C_3H_6), as well as hydrogen (H_2) are also present in the thickness of sedimentary rocks, the distributions of which are similar in the studied sections (Fig. 3).

Timofeev G. and Umnova N. [10] point to a low concentration of hydrocarbon gases in intervals with high hydrogen and unsaturated hydrocarbons and express the opinion that such distribution of gases is specific to the syngenet ic processes of the lithification of organic matter during gas generation.

They are also supported by F.A. Alekseev and others [11], who believe that the confinement of increased concentrations of unsaturated hydrocarbons to sandy clay bodies and the correlation of their sectional distribution in terms of hydrogen are indicators of the transformation of organic matter (OM).

In the component composition of hydrocarbon gas deposits, unsaturated hydrocarbons (UH) are virtually absent, so the ratio of their content to the concentration of hydrocarbon gases (UH/H) allows us to assume the predominance of syn- or epigenetic hydrocarbon fluids in the studied section.

The decreased content of hydrogen and unsaturated hydrocarbons is observed only at depth intervals where the gas saturation of rocks increases, which is associated with the flow of methane gas into their section, as evidenced by a significant increase in the CH_4/C_2-C_6 ratio (Fig. 3). It can be assumed that the decrease in the amount of hydrogen and unsaturated methane homologues is caused only by geochemical processes in which they are directly involved.

These processes are likely to be the interaction of hydrogen and unsaturated methane homologues to form ethane and propane and the interaction of hydrogen and nitrogen to form ammonium. They occur only in the gas phase and do not take place in the aqueous medium (Fig. 4a).

In the gas phase, molecules are in constant chaotic motion, colliding with each other. These collisions release energy, which causes molecules to interact with each other (Fig. 4b).

The movement of molecules in a liquid differs from that in gases: water molecules form an ordered structure due to hydrogen bonds (Fig. 4c), which makes it impossible for gas molecules to move chaotically, which excludes the interaction between hydrogen and unsaturated hydrocarbons, as well as between hydrogen and nitrogen.

Therefore, the flow of free methane gas into reservoir deposits results in gaseous fluid accumulation, which in turn creates the prerequisites for the interaction between hydrogen and unsaturated hydrocarbons or nitrogen. The absence of hydrogen in the context of productive oil and gas bearing structures is confirmed by the materials presented in works of G. Lebed' and others [12].

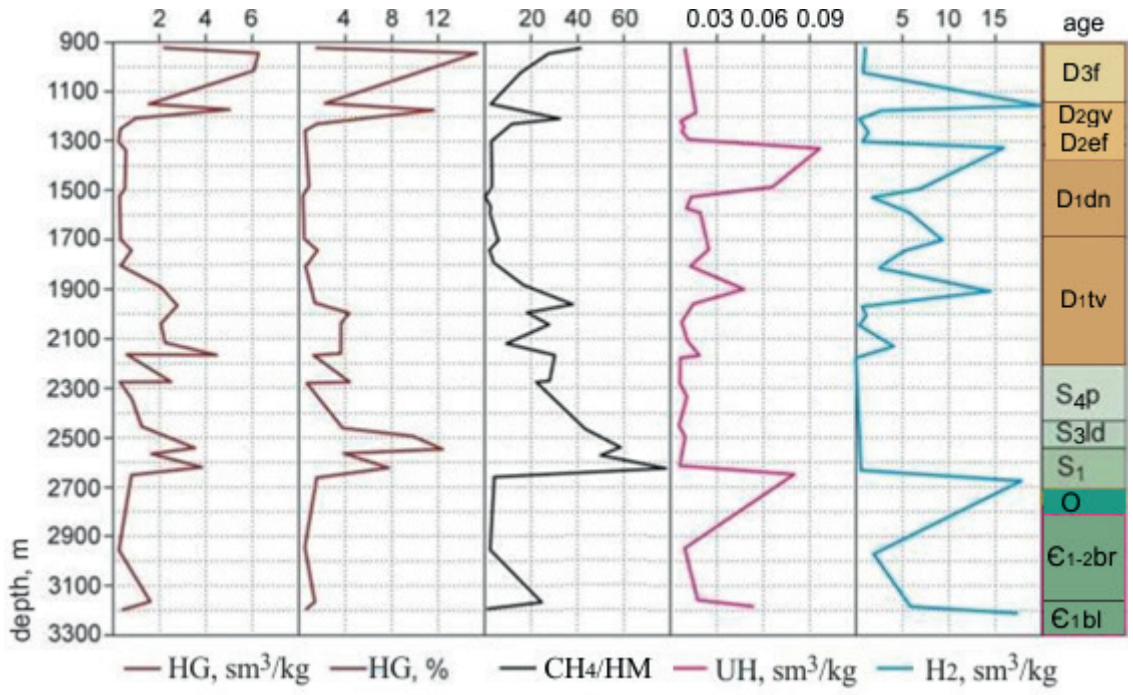

Fig. 3. Distribution of gas parameters in the Volyn-Podillya well based on the results of geochemical studies.
HG – hydrocarbon gases C_1-C_6; CH_4/HM – methane to homologues ratio; UH – unsaturated hydrocarbons; H_2 – hydrogen
D_3fr – Frasnian; D_2gv – Givetian; D_2ef – Eifelian; D_1dn – Dnisterska Series; D_1tv – Tiverska Series ; S_4p – Pridoli; S_3ld – Ludlow;
$Є_{1\text{-}2}$br – Berezskivska Series; $Є_1$bl – Baltic Series

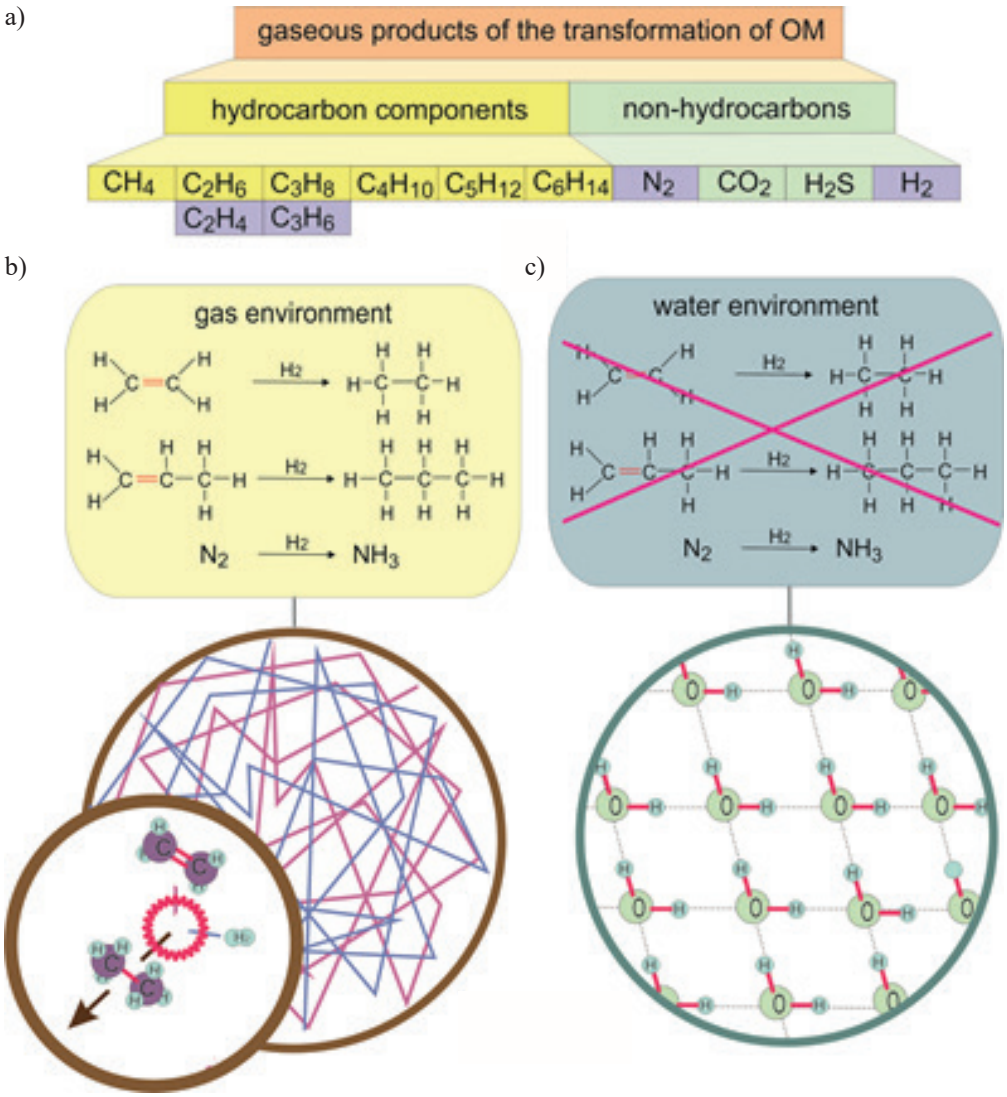

Fig. 4. Interaction of gaseous products of OM transformation depending on the nature of fluid saturation of the section (a); chaotic movement of molecules in the gas phase, interaction between them (b); hydrogen bonds between water molecules (c)

Based on the above materials, conclusions can be drawn about the distribution of gases, including hydrogen, in the sedimentary complex:

- Nitrogen is the main component of water-dissolved gases in formation waters of the sedimentary complex; towards the gas reservoir, the concentration of nitrogen decreases, but the concentration of ammonium increases.
- There is a similarity in the distribution of hydrogen and unsaturated hydrocarbons in well sections, the maximum content of the latter is confined to intervals with background hydrocarbon gases; in gas-saturated formations, the concentration of hydrogen and unsaturated methane homologues decreases significantly.
- The processes of the interaction of gaseous substances only occur in the gas phase and do not take place in the aqueous medium. Methane gas entering the sediments triggers the origination of a gas phase, i.e. an environment in which hydrogen interacts with both nitrogen and unsaturated hydrocarbons. The result of these processes is that the nitrogen content in formation water in the gas deposit zone is significantly reduced, and unsaturated hydrocarbons and hydrogen are absent in the component composition of the hydrocarbon accumulation.
- There is a similarity in the distribution of hydrogen and unsaturated hydrocarbons in well sections, the maximum content of the latter is confined to intervals with background hydrocarbon gases; in gas-saturated formations the concentration of hydrogen and unsaturated methane homologues is significantly reduced.

– The processes of interaction of gaseous substances occur only in the gas phase and do not take place in the aqueous medium. Methane gas entering the reservoirs leads to the formation of a gas phase in the reservoirs, an environment in which hydrogen interacts with both nitrogen and unsaturated hydrocarbons. As a result of these processes, the nitrogen content of produced water in the gas reservoir zone is significantly reduced, and unsaturated hydrocarbons and hydrogen are absent from the hydrocarbon accumulation.

4. Results of hydrogen research in Volyn-Podillya

There is no consensus on the sources of hydrogen. However, hydrogen is not only found in volcanic and metamorphic rocks, but also in sedimentary cover deposits; the latter, according to many researchers, is due to the catabolism of organic matter.

At present, there is only one known natural deposit of geological hydrogen (almost pure – 98% content) in the world – Burakebougou in Mali, which is unique in its nature and essence. The issue of the genesis of hydrogen in this field has not been fully clarified [13].

Taking into account the above patterns, we analyzed gas logging in the Lutsk-1 well, which was drilled to study the geological section of Palaeozoic-Proterozoic sediments and the prospects for their oil and gas content.

4.1. Geochemical studies of the Lutsk-1 well

The Lutsk-1 parametric well was drilled within the area of the same name on the northeastern side of the Lviv Palaeozoic trough to study the stratigraphy, oil and gas content and filtration capacity characteristics of Palaeozoic and Proterozoic sediments (Fig. 5a). During drilling, the Lutsk-1 well reached a depth of 2,442 m, having penetrated the crystalline basement rocks from the mark of 2,404 m (Fig. 5b).

According to the results of the core gas survey, the highest hydrocarbon saturation of rocks was determined in the Archean-Proterozoic sediments (int. 2,440.2–2,441.8 m) and at the boundary of the Middle and Lower Devonian (int. 309–318 m) (Fig. 6).

With regard to study findings, it should be noted that the hydrogen content in the studied gases, starting from the Cambrian sediments and down the section, significantly increases to 40% (Fig. 6), which exceeds the hydrocarbon concentration by 5–10 times.

It is observed that intervals with high hydrogen content are characterized as water-saturated and water-gas-saturated according to the data of reservoir testing (RST) and the results of geochemical studies (GC).

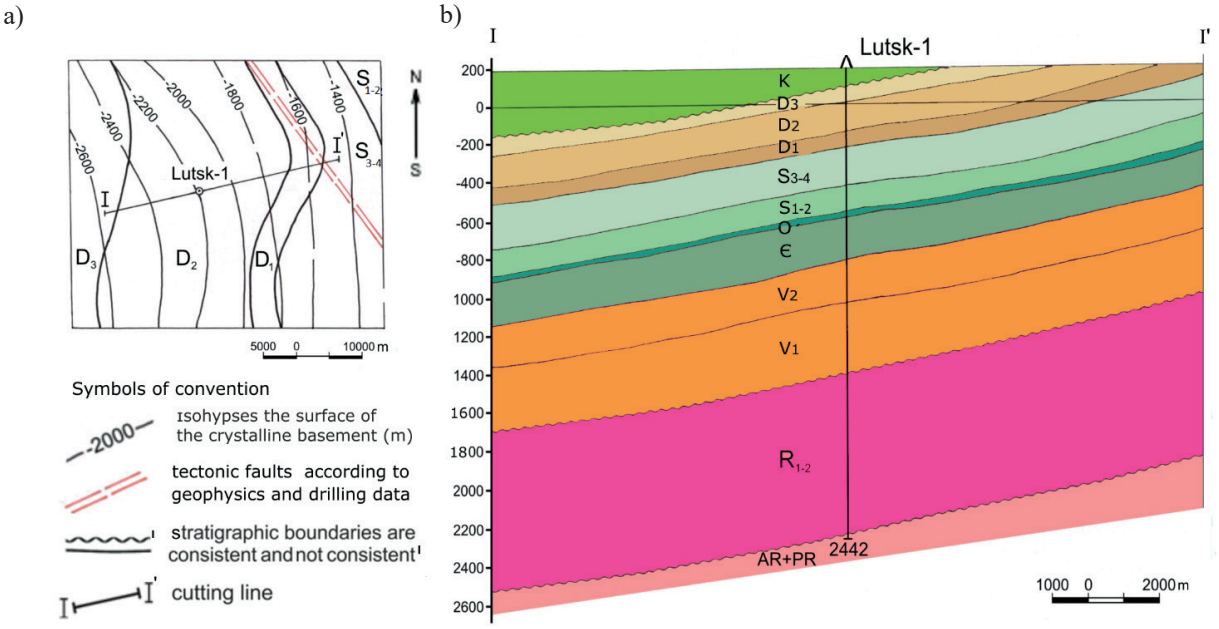

Fig. 5. Structural map of the crystalline basement roof (a) and geologic section along the I-I line (b) within the Lutsk area
D_3fr – Frasnian; D_2 (gv – Givetian, ef – Eifelian); D_1tv – Tiverska Series; S_{3-4} (p – Pridoli, ld – Ludlow);
Є ($Є_{1-2}$br – Berezskivska Series, $Є_1$bl – Baltic Series); V_2 (kn – Kaniliv Series, mp – Mogiliv-Podilska Series);
V_1 (brs – Berestovetska Suite, gr – Gorbaschivska Suite); R_{1-2} (pl – Polytska Suite, rm – Romeikivska Suite); AR-PR – metamorphic rocks

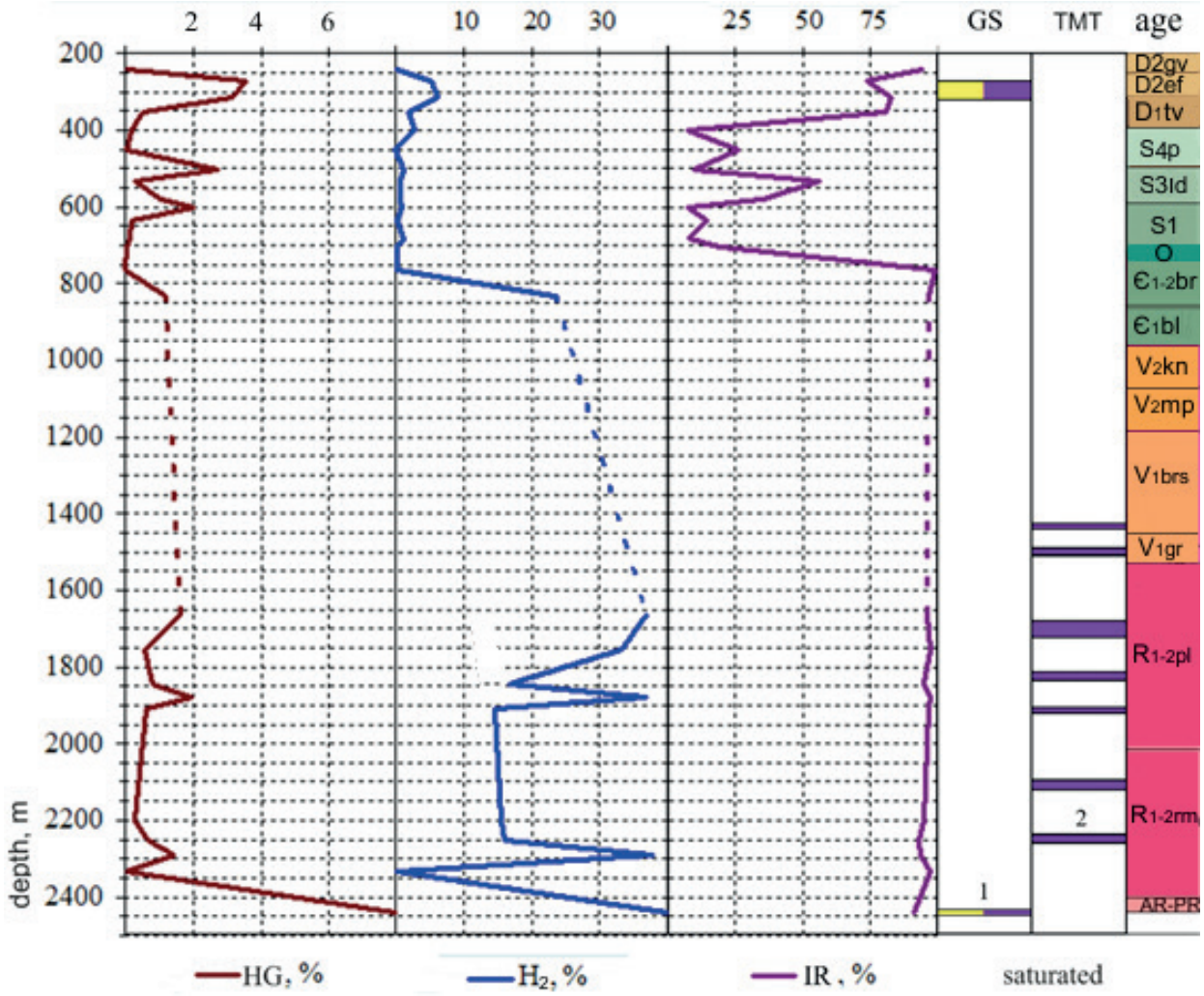

Fig. 6. Saturation pattern of the Lutsk-1 well section based on the results of geochemical studies (GS) and test materials (TMT). HG – hydrocarbon gases C_1-C_6, H_2 – hydrogen, IR – insoluble rock residue in HCl. Saturation: 1 – water and gas saturated, 2 – water-saturated D_2gv – Givetian; D_2ef – Eifelian; D_1tv – Tiverska Series; S_4p – Pridoli; S_3ld – Ludlow; $Є_{1-2}$br – Berezskivska Series; $Є_1$bl – Baltic Series; V_2kn – Kaniliv Series; V_2mp – Mogiliv-Podilska Series; V_1brs – Berestovetska Suite; V_1gr – Gorbaschivska Suite; R_{1-2}pl – Polytska Suite; R_{1-2}rm – Romeikivska Suite; AR-PR – metamorphic rocks

5. Conclusions

Based on the above materials, it is possible to draw conclusions about the need to study the distribution of gases, including hydrogen, in the sedimentary section of the studied areas.

Taking into account the above-mentioned regularities, we analyzed gas logging in the Lutsk-1 well, which was drilled to study the geological section of Palaeozoic--Proterozoic sediments and the prospects for their oil and gas content.

According to the results of geophysical surveys, all the selected layers in the well section are watered, and the best reservoir properties are in the Cambrian and Riphean sandstones.

The core gasometric studies indicate that the highest hydrocarbon saturation of rocks is found in the Archean-Proterozoic sample in the interval of 2,440–2,442 m.

However, it should be noted that in the context of Proterozoic and Cambrian rocks, the hydrogen content in the component composition of gases absorbed by rocks increases significantly, which significantly exceeds the hydrocarbon concentration (Fig. 6). Of note is that the intervals with high hydrogen content, according to the data of reservoir testing (RST) and the results of geochemical studies (GC), are estimated as water-saturated and water-gas-saturated. This correlates with the data of the University of Lorraine, which found hydrogen gas bubbles in a water-saturated section [1].

Hydrogen was detected in many wells in the Volyn-Podillya region of Ukraine based on the results of core sampling. Generalization of the results of hydrogen distribution in these wells will allow us to further identify zones characterized by high hydrogen content as well as to establish geological and structural elements to which the increased hydrogen content in the rock section is confined. The obtained materials will allow directions for the search for hydrogen in the sedimentary cover within the territory of Volyn-Podillya to be established.

References

[1] *It Could Be a Vast Source of Clean Energy, Buried Deep Underground*. The New York Times, 4.12.2023. https://www.nytimes.com/2023/12/04/business/energy-environment/clean-energy-hydrogen.html [20.12.2023].

[2] Konoplyova M.: *Deposits of pure hydrogen discovered in Rivne region*, 2020. https://shotam.info/na-rivnenshchyni-znaysh-ly-rodovyshcha-chystoho-vodniu/ [20.10.2023].

[3] *Energy balance of Ukraine*, 2022. https://stat.gov.ua/uk/datasets/enerhetychnyy-balans-ukrayiny-0 [20.10.2023].

[4] Zorkyn L.M.: *Geokhimiya gazov plastovykh vod neftegazonosnykh basseynov.* Nedra, Moskva 1973 [Зорькин Л.М.: *Геохимия газов пластовых вод нефтегазоносных бассейнов*. Недра, Москва 1973].

[5] Gatalskyi M.A.: *Podzemnyye vody Belorussii v svyazi s otsenkoy perspektiv yeyeneftegazonosnosti.* In: *Geologiya, gidrogeologiya i neftegazonosnost'.* Gostoptekhizdat, Minsk 1963, pp. 165–314 [Гатальский М.А.: *Подземные воды Белоруссии в связи с оценкой перспектив ее нефтегазоносности.* В: *Геология, гидрогеология и нефтегазоносность*. Гостоптехиздат, Минск 1963, С. 165–314].

[6] Shvai L.P.: *Podzemnyye vody Dneprovsko-Donetskoy vpadiny v svyazi s neftegazonosnost'yu* Nedra, Moskva 1973 [Швай Л.П.: *Подземныые воды Днепровско-Донецкой впадины в связи с нефтегазоносностью*. Недра, Москва 1973].

[7] Kolodii V.V.: *Naftohazova hidroheolohiia: pidruchnyk*. IFNTUNG Fakel, Ivano-Frankivsk, 2009 [Колодій В.В.: *Naftogazova gidrogeologiya: pidruchnik*. ІФНТУНГ Факел, Івано-Франківськ 2009].

[8] Hunt J.M.: *Petroleum Geochemistry and Geology*. W.H. Freeman, Oxford 1979.

[9] Gavrish V.K.: *Rol' hlybynnykh rozlomiv u mihratsiyi ta akumulyatsiyi nafty ta hazu*. Naukova dumka, Kyiv 1978 [Гавриш В.К.: *Роль глубинных разломов в миграции и аккумуляции нефти и газа. Наукова думка*, Киев 1978, С. 32].

[10] Timofeyev G.I., Umnova N.V.: *Ispol'zovaniye gazov zakrytykh por dlya prognozirovaniya gazonosnosti karbonatnykh otlozheniy*. In: *Neftyanaya promyshlennost', seriya neftegazovaya geologiya,geofizika i bureniye*. Nedra, Moskva 1984, Vyp. 10. pp. 13–16 [Тимофеев Г.И., Умнова Н.В.: *Использование газов закрытых пор для прогнозирования газоносности карбонатных отложений. В: Нефтяная промышленность, серия нефтегазовая геология, геофизика и бурение*. Недра, Москва 1984, Вып. 10, С. 13–16].

[11] Alekseyev F.A., Porshn′ova N.St., Stklyanyn Y.I., Slavina H.P.: *Pryamyye geokhimicheskiye metody poiska neftyanykh i gazovykh mestorozhdeniy.* In: *Problema geokhimicheskikh poiskov neftyanykh i gazovykh mestorozhdeniy i voprosov yadernoy geologii*. Nedra, Moskva 1968, Vyp. 4, pp. 5–57 [Алексеев Ф.А., Поршнева Н.В., Стклянин Ю.И., Славина Г.П.: *Прямые геохимические методы поисков нефтяных и газовых месторождений. Проблема геохимических поисков нефтяных и газовых месторождений и вопросы ядерной геологии*. Недра, Москва 1968. Вып. 4, С. 5–57].

[12] Lebed' G.G., Mal'denbaum M.M., Obukhovich G.A. et al.: *Metodika rezul'tatov i poisk nefti i gaza na yuge Sibirskoy platformy.* In: *Geokhimicheskiye* metody *poiskov mestorozhdeniy nefti i gaza*. Nauka, Kyiv 1983, pp. 101–109 [Лебедь Г.Г.: Мальденбаум М.М., Обухович Г.А. и др.: *Методика и результаты поисков нефти и газа на юге Сибирской платформы. В: Геохимические методы поисков месторождений нефти и газа. Наука*, Киев 1983, С. 101–109].

[13] Bezruchko K.A., *Natural sources and conditions of geological hydrogen formation (in the context of hydrogen deposits search)*. Geophysical Journal, 2, 44, 2022, pp. 93–124. https://doi.org/10.24028/gj.v44i2.256267.

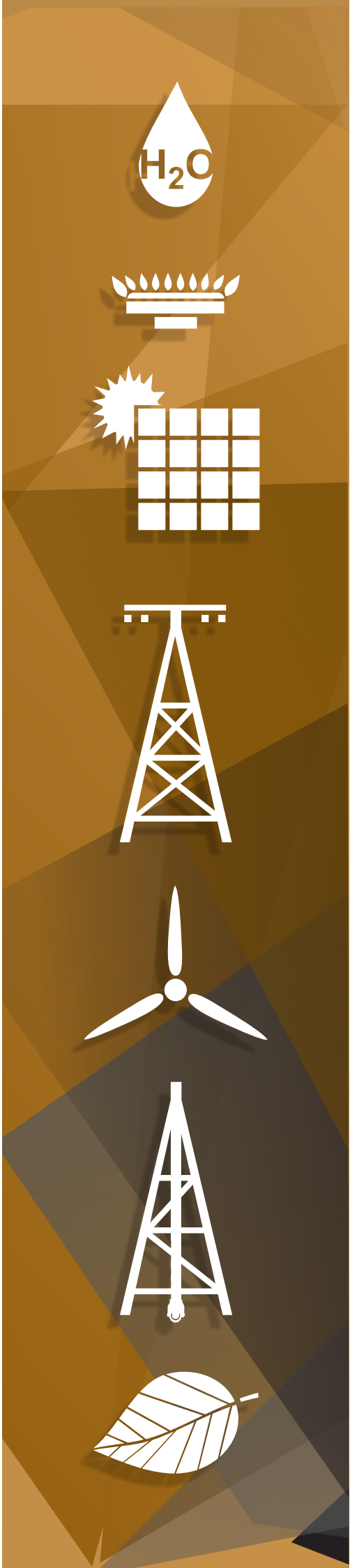
H2O